Beyond Affinity: A Benchmark of 1D, 2D, and 3D Methods Reveals Critical Trade-offs in Structure-Based Drug Design

Anonymous authors
Paper under double-blind review

Abstract

Currently, the field of structure-based drug design is dominated by three main types of algorithms: search-based algorithms, deep generative models, and reinforcement learning. While existing works have typically focused on comparing models within a single algorithmic category, cross-algorithm comparisons remain scarce. In this paper, to fill the gap, we establish a benchmark to evaluate the performance of fifteen models across these different algorithmic foundations by assessing the pharmaceutical properties of the generated molecules and their docking affinities and poses with specified target proteins. We highlight the unique advantages of each algorithmic approach and offer recommendations for the design of future SBDD models. We emphasize that 1D/2D ligand-centric drug design methods can be used in SBDD by treating the docking function as a black-box oracle, which is typically neglected. Our evaluation reveals distinct patterns across model categories. 3D structure-based models excel in binding affinities but show inconsistencies in chemical validity and pose quality. 1D models demonstrate reliable performance in standard molecular metrics but rarely achieve optimal binding affinities. 2D models offer balanced performance, maintaining high chemical validity while achieving moderate binding scores. Through detailed analysis across multiple protein targets, we identify key improvement areas for each model category, providing insights for researchers to combine strengths of different approaches while addressing their limitations.

1 Introduction

Novel types of safe and effective drugs are needed to meet the medical needs of billions worldwide and improve the quality of human life. The process of discovering a new drug candidate and developing it into an approved drug for clinical use is known as *drug discovery* (Sinha & Vohora, 2018). This complex process is fundamental to the development of new therapies that can manage, cure, or alleviate the symptoms of various health conditions.

Structure-based drug design (SBDD) (Bohacek et al., 1996) is a core strategy that accelerates this process by using the three-dimensional (3D) structures of disease-related proteins to develop drug candidates. This approach is grounded in the "lock and key" model (Tripathi & Bankaitis, 2017), where molecules that bind more effectively to a target protein are more likely to modulate its function, a principle validated by numerous experimental studies (Honarparvar et al., 2014; Blundell, 1996; Lu et al., 2022).

Currently, three main algorithmic approaches dominate the drug design field (Brown et al., 2019; Gao et al., 2022; Du et al., 2022): search-based algorithms like genetic algorithms (GA) (Jensen, 2019; Spiegel & Durrant, 2020; Tripp & Hernández-Lobato, 2023; Fu et al., 2022a), deep generative models such as variational autoencoder (VAE) (Gómez-Bombarelli et al., 2018) and autoregressive models (Luo et al., 2021; Peng et al., 2022; Zhang et al., 2023), and reinforcement learning (RL) models (Olivecrona et al., 2017; Zhou et al., 2019). While these models, particularly those using 3D protein representations (Zhang et al., 2023; Luo et al., 2021; Fu et al., 2022a; Peng et al., 2022), are considered state-of-the-art for generating valid and diverse molecules, a clear comparative understanding across these different algorithmic foundations is lacking. Existing benchmarks often focus on comparing models within the same category (typically deep generative

Table 1: Representative structure-based drug design methods, categorized based on the molecular assembly strategies and the optimization algorithms. Columns are various molecular assembly strategies while rows are different optimization algorithms.

	1D SMILES/SELFIES	2D Molecular Graph	3D Structure-based
Genetic Algorithm (GA)	SMILES-GA (Yoshikawa et al., 2018)	Graph GA (Jensen, 2019)	-
Hill Climbing	SMILES-LSTM-HC (Brown et al., 2019)	MIMOSA (Fu et al., 2021)	-
Reinforcement Learning (RL)	REINVENT (Olivecrona et al., 2017)	MolDQN (Zhou et al., 2019)	-
Gradient Ascent (GRAD)	Pasithea (Shen et al., 2021)	DST (Fu et al., 2022b)	-
Generative Models	SMILES/SELFIES-VAE-BO (Gómez-Bombarelli et al., 2018)	JT-VAE (Jin et al., 2019)	3DSBDD (Luo et al., 2021), Pocket2mol (Peng et al., 2022), Pocket-Flow (Jiang et al., 2024), ResGen (Zhang et al., 2023), TargetDiff (Guan et al., 2023)

Table 2: Top 1 docking score for each target. Targets in CrossDocking are marked in red, and targets not in CrossDocking are in blue.

Model	6GL8	1UWH	7OTE	1KKQ	5WFD	7W7C	8JJL	7D42	7S1S	6AZV
Pocket2Mol	**-11.56**	**-14.56**	**-15.72**	**-14.18**	-11.30	-13.76	**-13.27**	-12.76	**-12.90**	**-12.36**
PocketFlow	-9.42	-11.04	-10.27	-12.47	-10.30	-13.52	-11.88	**-12.79**	-10.16	-11.83
ResGen	–	-9.71	-7.14	-9.81	–	-7.88	–	-8.94	-11.77	-9.71
3DSBDD	-8.61	-12.67	-10.52	-13.36	-11.28	-11.29	-11.67	-11.12	-10.19	-10.13
DST	-8.69	-11.09	-11.41	-10.92	-10.13	-12.14	-12.20	-11.87	-11.54	-10.31
graph-GA	-8.47	-11.19	-11.15	-10.61	-9.66	-11.85	-10.72	-11.03	-10.47	-9.85
JT-VAE	-10.26	-12.38	-12.29	-12.25	**-11.65**	-12.45	-11.91	**-12.79**	-11.53	-10.60
MIMOSA	-8.64	-11.13	-11.49	-11.00	-9.91	-11.72	-11.85	-11.72	-11.96	-10.27
MolDQN	-6.63	-7.38	-7.49	-7.35	-7.79	-7.75	-8.94	-7.30	-8.42	-8.04
Pasithea	-9.25	-11.47	-11.56	-10.45	-10.54	-12.00	-11.87	-11.76	-11.35	-10.24
REINVENT	-9.06	-11.13	-12.03	-11.19	-10.18	-11.88	-11.63	-12.23	-11.32	-10.66
SMILES-GA	-8.83	-10.74	-11.18	-10.47	-9.72	-11.74	-11.29	-11.93	-11.05	-10.46
SMILES-LSTM-HC	-9.77	-11.50	-12.35	-12.40	-11.21	**-13.93**	-11.41	-12.84	-12.02	-10.61
SMILES-VAE	-9.35	-11.95	-13.06	-10.91	-10.01	-12.11	-11.95	-12.01	-12.14	-10.42
TargetDiff	–	-7.30	–	-11.53	-10.07	-9.27	-8.91	-6.10	–	–

models) and prioritize molecular properties over the crucial evaluation of protein-ligand interactions. (Du et al., 2022; Brown et al., 2019; Gao et al., 2022).

To fill this blank, this paper curates a comprehensive benchmark that encompasses fifteen models spanning all three algorithmic approaches. We assess model performance through multiple dimensions: traditional heuristic molecular property oracles, docking scores, and pose evaluations - all critical metrics for understanding the quality of protein-ligand interactions in the context of drug discovery. Our analysis reveals a notable dichotomy in 3D models' performance: while they excel in docking score optimization, achieving consistently superior binding affinity predictions, they show comparable or sometimes inferior performance in pose quality assessments and other heuristic property evaluations. These findings highlight the need for future structure-based models to better balance docking score optimization with other crucial molecular properties and structural validity metrics.

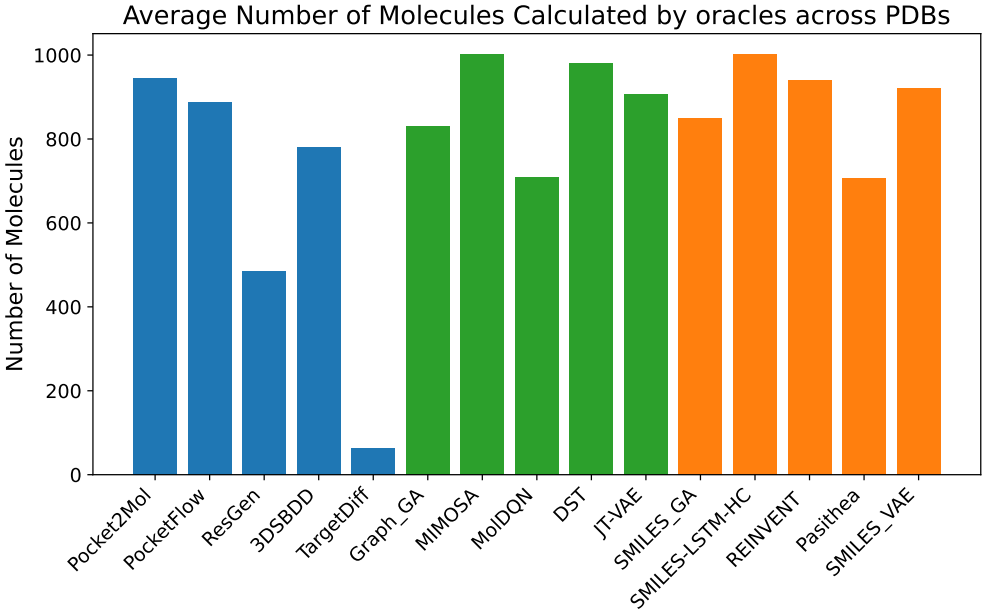

Figure 1: The bar chart of average generated molecules that are calculated by our selected oracles for each model across all target proteins under given time. 1D methods are colored orange, blue is used to indicate 3D methods, and green represents 2D methods.

2 Related Works

Significant progress has been made in benchmarking drug design models (Brown et al., 2019; Tripp et al., 2021; Huang et al., 2021; Gao et al., 2022; Polykovskiy et al., 2020; Harris et al., 2023). Benchmarks like Guacamol, Molecular Sets (MOSES), Practical Molecule Optimization (PMO), and POSECHECK have been crucial for evaluating algorithms on molecular properties and protein-ligand interactions. Building on this, our work provides a cross-algorithmic comparison of fifteen models, which we group into three categories based on their molecular representation.

1D Molecule Design Methods 1D molecule design methods use Simplified Molecular-Input Line-Entry System (SMILES) (Weininger, 1988) or SELF-referencing Embedded Strings (SELFIES) (Lo et al., 2023) strings as the representation of molecules. Most 1D methods produce molecule strings in an autoregressive manner. In this paper, we discuss several methods that were developed to produce molecule strings, either SMILES or SELFIES strings, including REINVENT (Olivecrona et al., 2017), SMILES and SELFIES VAE (Gómez-Bombarelli et al., 2018), SMILES GA (Yoshikawa et al., 2018), SMILES-LSTM-HC (Brown et al., 2019), and Pasithea (Shen et al., 2021). Although SELFIES string has the advantage of enforcing chemical validity rules compared to SMILES, through thorough empirical studies, Gao et al. (2022) showed that SELFIES string-based methods do not demonstrate superiority over SMILES string-based ones.

2D Molecule Design Methods Compared to 1D molecule design methods, representing molecules using 2D molecular graphs is a more sophisticated approach. molecular 2D representation, graphs are used to depict molecules, where edges represent chemical bonds and nodes represent atoms. There are two main strategies for constructing these graphs: atom-based and fragment-based. Atom-based methods operate on one atom or bond at a time, searching the entire chemical space. On the other hand, fragment-based methods summarize common molecular fragments and operate on one fragment at a time, which can be more efficient. In this paper, we discuss several methods belonging to this category: MolDQN (Zhou et al., 2019), which uses an atom-based strategy, and Graph GA (Jiang et al., 2024), Multi-constraint Molecule Sampling (MIMOSA) (Fu et al., 2021), Differentiable Scaffolding Tree (DST) (Fu et al., 2022b), JT-VAE (Jin et al., 2019) which use fragment-based.

3D Molecule Design Methods Both 1D and 2D molecule design methods are ligand-centric, focusing primarily on designing the molecule itself. In structure-based drug design, as pointed out in Huang et al. (2021), these models take the docking function as a black box, which inputs a molecule and outputs the binding affinity score. However, these models fail to incorporate target protein structure information and consequently suffer from high computational time (to find binding pose). In contrast, 3D structure-based drug design methods take the three-dimensional geometry of the target protein as input and directly generate pocket-aware molecules in the pocket of target protein. In this paper, we cover five cutting-edge structure-based drug design methods: TargetDiff (Guan et al., 2023), PocketFlow (Jiang et al., 2024), 3DSBDD (Luo et al., 2021), Pocket2mol (Peng et al., 2022), and ResGen (Zhang et al., 2023).

3 Models

In this paper, the models we select for evaluation are based on one or a combination of the following algorithms. For ease of comparison, we categorize all the methods based on optimization algorithm and molecular assembly strategy in Table 1.

Genetic Algorithm (GA): Inspired by natural selection, genetic algorithm is a combinatorial optimization method that evolves solutions to problems over many generations. Specifically, in each generation, GA will perform crossover and mutation over a set of candidates to produce a pool of offspring and keep the top-k offspring for the next generation, imitating the natural selection process. In our evaluation, we choose three GA models: SMILES GA (Yoshikawa et al., 2018) that performs GA over SMILES string-based space, Graph GA (Jiang et al., 2024) that searches over atom- and fragment-level by designing their crossover and mutation rules on graph matching.

Variational Auto-Encoder (VAE) and Diffusion: The aim of variational autoencoder is to generate new data that is similar to training data. In the molecule generation area, VAE learns a bidirectional map between molecule space and continuous latent space and optimizes the latent space. VAE itself generated diverse molecules that are learned from the training set. After training VAE, Bayesian optimization (BO) is used to navigate latent space efficiently, identify desirable molecules, and conduct molecule optimization. In our evaluation, we select three VAE-based models and one diffusion-based model: SMILES-VAE-BO (Gómez-Bombarelli et al., 2018) uses SMILES string as the input to the VAE model, and SELFIES-VAE-BO uses the same algorithm but uses SELFIES string as the molecular representation. JT-VAE (Jin et al., 2019) instead use a tree-structured scaffold over chemical substructures. TargetDiff (Guan et al., 2023) design a target-aware diffusion model that could generate molecules under given protein atoms.

Auto-regressive: An auto-regressive model is a type of statistical model that is based on the idea that past values in the series can be used to predict future values. In molecule generation, an auto-regressive model would typically take the generated atom sequence as input and predict which atom would be the next. In our evaluation, we choose seven auto-regressive models: PocketFlow (Jiang et al., 2024) is autoregressive flow-based generative models. 3DSBDD (Luo et al., 2021) based on conventional Markov Chain Monte Carlo (MCMC) algorithms and Pocket2mol (Peng et al., 2022) choose graph neural networks (GNN) as the backbone. Inspired by Pocket2mol, ResGen (Zhang et al., 2023) used a hierarchical autoregression, which consists of a global autoregression for learning protein-ligand interactions and atomic component autoregression for learning each atom's topology and geometry distributions.

Hill Climbing (HC): Hill Climbing (HC) is an optimization algorithm that belongs to the family of local search techniques (Selman & Gomes, 2006). It is used to find the best solution to a problem among a set of possible solutions. In molecular design, Hill Climbing would tune the generative model with the reference of generated high-scored molecules. In our evaluation, we adopt two HC models: SMILES-LSTM-HC (Brown et al., 2019) uses an LSTM model to generate molecules and uses the HC technique to fine-tune it. MultI-constraint MOlecule SAmpling (MIMOSA) (Fu et al., 2021) uses a graph neural network instead and incorporates it with HC.

Gradient Ascent (GRAD): Similar to gradient descent, gradient ascent also estimates the gradient direction but chooses the maximum direction. In molecular design, the GRAD method is often used in molecular property function to optimize molecular generation. In our evaluation, we choose two GRAD-based models:

Pasithea (Shen et al., 2021) uses SELFIES as input and applies GRAD on an MLP-based molecular property prediction model. Differentiable Scaffolding Tree (DST) (Fu et al., 2022b) uses differentiable molecular graph as input and uses a graph neural network to estimate objective and the corresponding gradient.

Reinforcement Learning (RL): In molecular generation context, a reinforcement learning model would take a partially-generated molecule (either sequence or molecular graph) as state; action is how to add a token or atom to the sequence or molecular graph respectively; and reward is the property score of current molecular sequence. In our evaluation, we test on two RL-based models: REINVENT (Olivecrona et al., 2017) is a policy-gradient method that uses RNN to generate molecules and MolDQN (Zhou et al., 2019) uses a deep Q-network to generate molecular graph.

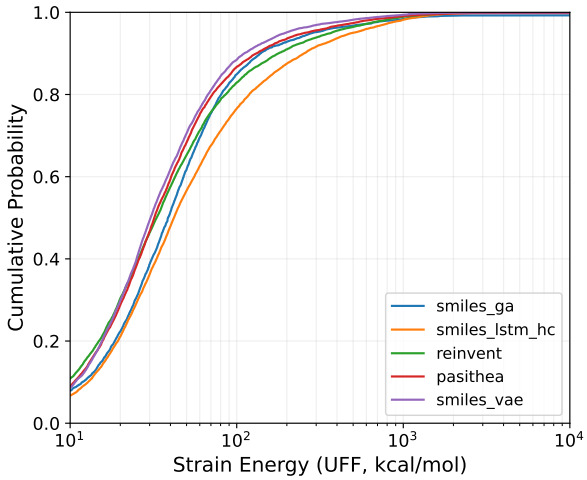

(a) 1D models

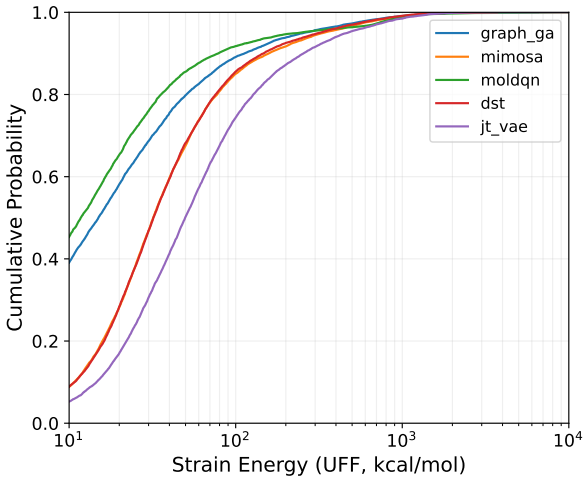

(b) 2D models

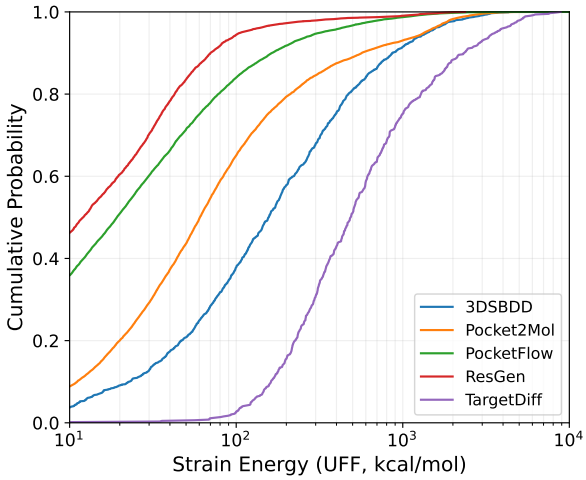

(c) 3D models

Figure 2: The cumulative density function (CDF) of strain energy of each model

4 Experiments

In this section, we demonstrate the experimental results. We start with the description of experimental setup. Then, we present and analyze the experimental results, including protein-ligand bindings and pose, pharmaceutical properties of generated molecules (e.g., drug-likeness and synthetic accessibility), and other qualities of generated molecules (e.g., diversity, validity).

4.1 Experiment Setup

4.1.1 Oracle

In drug discovery, we need to evaluate the pharmaceutical properties of the generated molecules, such as binding affinity to certain target proteins, drug-likeness, synthetic accessibility, solubility, etc. These property evaluators are also known as *oracle*. In this section, we introduce the oracle we chose to evaluate these models. The oracle functions are sourced from either the Therapeutics Data Commons (TDC) (Huang et al., 2022; 2021)[1] or established Python packages.

(1) Docking Score: Molecular docking is a measurement of free energy exchange between a ligand and a target protein during the binding process. A lower docking score means the ligand would have a higher potential to pose higher bioactivity with a given target. Compared with other heuristic oracles, such as QED (quantitative estimate of drug-likeness), and LogP (Octanol-water partition coefficient), docking reflects the binding affinities between drug molecule and target (Graff et al., 2021). Our experiments use AutoDock Vina (Eberhardt et al., 2021) python package to calculate the docking score for each generated molecules. We selected ten representative and diverse target proteins, with five sourced from CrossDock (Francoeur et al., 2020) and five from other datasets. The CrossDock-derived PDB IDs are 6GL8, 1UWH, 7OTE, 1KKQ, and 5WFD, while the remaining structures are 7WC7, 8JJL, 7D42, 6AZV, and 7S1S. These crystallography structures are across different fields, including virology, immunology, and oncology (Huang et al., 2022; 2021; Chang et al., 2019). They cover various kinds of diseases such as chronic myelogenous leukemia, tuberculosis, SARS-COVID-2, etc. They represent a breadth of functionality, from viral replication mechanisms to cellular signaling pathways and immune responses.

(2) Pose: Pose evaluation is another crucial oracle in structure-based drug discovery. It primarily focuses on measuring physical and chemical validity aspects of docking, such as chemical consistency, geometric plausibility, and energy-based checks. These assessments help eliminate physically implausible poses that might score well in Vina but are chemically or geometrically invalid. Additionally, it evaluates intermolecular interactions between the ligand and protein, such as steric clashes, to ensure that the predicted poses are not only energetically favorable but also physically realistic in the protein environment. In our experiments, we employed two pose evaluation packages: PoseBuster (Buttenschoen et al., 2024) and PoseCheck (Harris et al., 2023). PoseBuster contains 19 True/False-style metrics spanning chemical validity and consistency, intramolecular validity, and intermolecular validity. PoseCheck provides numerical values for clashes and strain energy for each docking pose generated by Vina.

(3) Heuristic Oracles: Although heuristic oracles are considered to be "trivial" and too easily optimized, we still incorporate some of them into our evaluation metrics for comprehensive analysis. In our experiments, we utilize Quantitative Estimate of Drug-likeness (QED), SA, and LogP as our heuristic oracles. QED evaluates a molecule's drug-likeness on a scale from 0 to 1, where 0 indicates minimal drug-likeness and 1 signifies maximum drug-likeness, aligning closely with the physicochemical properties of successful drugs. SA, or Synthetic Accessibility, assesses the ease of synthesizing a molecule, with scores ranging from 1 to 10; a lower score suggests easier synthesis. LogP measures a compound's preference for a lipophilic (oil-like) phase over a hydrophilic (water-like) phase, essentially indicating its solubility in water, where the optimal range depends on the type of drug. But mostly the value should be between 0 and 5.

(4) Molecule Generation Oracles: While docking score oracles and heuristic oracles focus on evaluating individual molecules, molecule generation oracles assess the quality of all generated molecules as a whole. In our experiments, we choose three metrics to evaluate the generated molecules of each model: diversity, validity, and uniqueness. Diversity is measured by the average pairwise Tanimoto distance between the Morgan fingerprints (Benhenda, 2017). Validity is determined by checking atoms' valency and the consistency of bonds in aromatic rings using RDKit's molecular structure parser (Polykovskiy et al., 2020). Uniqueness is measured by the frequency at which a model generates duplicated molecules, with lower values indicating more frequent duplicates (Polykovskiy et al., 2020).

[1] `https://tdcommons.ai/functions/oracles/`

4.1.2 Model Setup

Inspired by Liu et al. (2024), we setup our experiment as follow: For each model, we aim to generate 1,000 molecules for each given target protein. In case there are models fail to sample sufficient enough molecules at one run, we will rerun models that failed at most three times with different seed. We do not retrain each model and instead we directly use the checkpoints they provided. We use the receptor information from Liu et al. (2024) when setting target. After we get enough molecules for each model, we apply the four oracles mentioned above to every molecule and collect the results. None of the tested models have prior knowledge of these oracle functions.

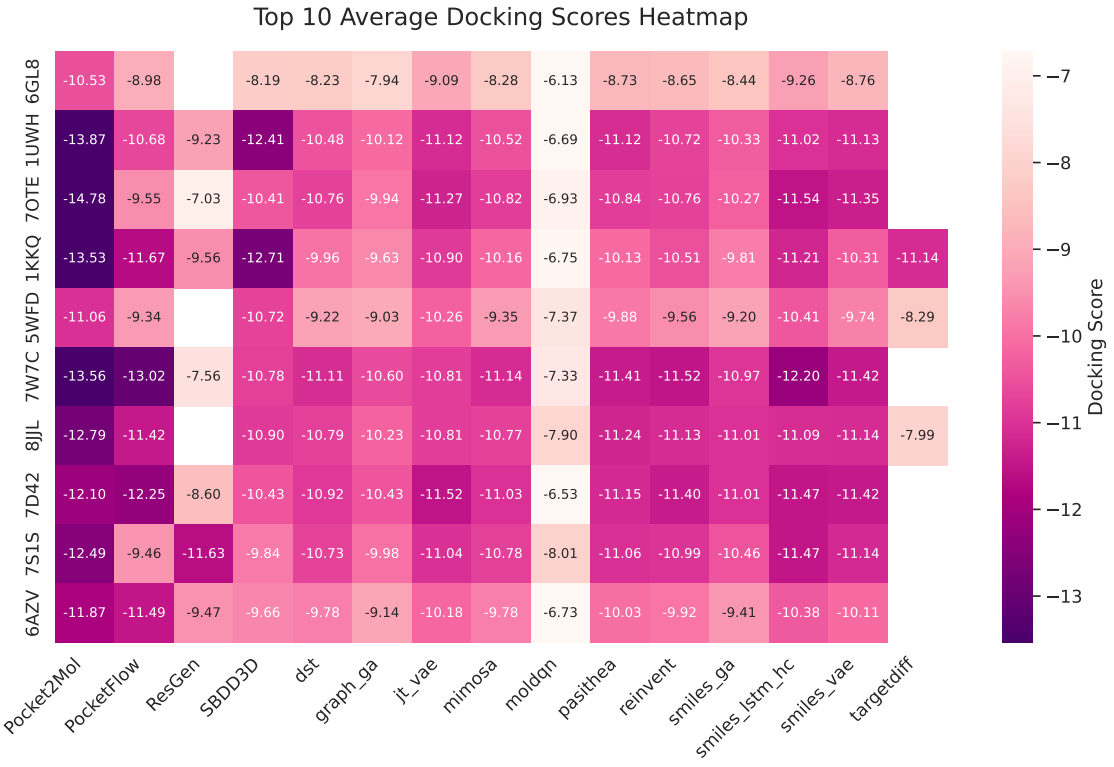

Figure 3: The heatmap based on the average of each model's Top-10 docking score for each target protein.

4.2 Experiment Results

In this section, we present our experimental results. First, we analyze the generation performance of each model, including the number of molecules successfully generated and stored, as well as generation speed. We then evaluate the oracle results for the generated molecules. Finally, we discuss our observations regarding model performance based on these analyses.

4.2.1 Generation Performance and Efficiency

In our analysis of model generation capabilities, we examined both generation speed and the total number of successfully stored molecules. As specified in the model setup section, each model was tasked with generating 1,000 molecules per run. We measured generation speed in molecules per minute, calculated by dividing the total generation time by 1,000. The speed results are presented in Table **??**.

Several models encountered execution issues with specific targets, resulting in 'error' designations. These failures occurred for three primary reasons: immediate execution errors (as with Pasithea), infinite loop conditions (as observed with MolDQN), and initialization failures due to unsuitable molecular configurations

(as seen with ResGen). It is important to note that the absence of recorded time does not necessarily indicate a complete failure to generate and store molecules.

Among successfully executing models, we first examined 1D and 2D models from the PMO benchmark (Gao et al., 2022), which underwent identical processing. Most of these models achieved average speeds of 1-3 molecules per minute. SMILES-GA demonstrated superior performance with speeds of 6-7 molecules per minute, followed by Graph-GA at 3-4 molecules per minute. The relatively modest speeds may be attributed to the computational overhead of PMO's internal oracle calculations, particularly for complex molecular structures.

In the 3D model category, ResGen achieved the highest average speed of approximately 300 molecules per minute. However, it failed to initiate generation for several targets (6GL8, 5WFD, 1UWH) given our receptor specifications. Pocket2mol maintained the second-highest performance at 40-60 molecules per minute, while PocketFlow operated at approximately 30 molecules per minute.

Regarding the number of stored molecules (Table 5), several models consistently approached or reached the 1,000-molecule target. SMILES-LSTM-HC, REINVENT, MIMOSA, and PocketFlow demonstrated notably stable performance, consistently generating and storing the full 1,000 molecules across most targets. However, some models showed significant variability. TargetDiff particularly struggled, storing fewer than 100 molecules for most targets, with its best performance being 557 molecules for 1KKQ. JT-VAE showed inconsistent performance, notably generating only 200 molecules for receptor 7WC7 despite strong performance with other targets. 3DSBDD displayed varying success rates, ranging from 222 to 1,000 stored molecules across different targets.

4.2.2 Binding Affinities and Poses

Method	Median Strain
graph-GA	14.99
MIMOSA	32.01
MolDQN	11.75
DST	32.06
JT-VAE	49.70
SMILES-GA	38.66
SMILES-LSTM-HC	41.95
REINVENT	33.11
Pasithea	31.99
SMILES-VAE	30.35
3DSBDD	157.11
Pocket2Mol	60.55
PocketFlow	19.21
ResGen	12.05
TargetDiff	487.72

Table 3: Median strain energies across different methods.

We first take a look about the docking score performance by the Top-1 (Table 2), Top-10 average (Table 6 and Figure 3) and Top-100 average (Table 7). Overall, the docking scores generally range from -14 to -5, with more negative values indicating better binding affinity. Pocket2Mol consistently demonstrates superior performance across all three tables, with score ranging from between -10 and -15. In contrast, MolDQN shows the weakest performance, with scores consistently around -5 to -7. The remaining models typically score between -8 and -12, with 3D models generally achieving the best scores across most targets.

1D models: The 1D models (SMILES-GA, SMILES-LSTM-HC, REINVENT, SMILES-VAE) show consistent performance across targets. In particular, SMILES-VAE and REINVENT demonstrate strong results with scores around -10 to -11 in the Top-10 average. SMILES-LSTM-HC exhibits slightly better perfor-

mance for CrossDocking targets compared to non-CrossDocking ones. SMILES-GA maintains performance comparable to other 1D models but shows higher variability across different targets.

2D models: The 2D models exhibit more diverse performance patterns compared to 1D models. DST and MIMOSA achieve scores comparable to 1D models, demonstrating competitive performance. Graph-GA maintains consistency but performs slightly below the top 1D models. JT-VAE scores well but shows notable variance across targets. MolDQN consistently underperforms relative to other 2D approaches.

3D models: Among 3D models, Pocket2Mol emerges as the clear leader, consistently achieving top scores. PocketFlow also performs strongly but shows higher variance between targets. ResGen delivers moderate but consistent performance. 3DSBDD displays the most variable performance among 3D models, achieving some excellent scores but with significant variance.

The above analysis demonstrates that while 3D models, particularly Pocket2Mol, can achieve the best overall scores, each category of models has its distinct performance characteristics and trade-offs.

We next examine the pose-related results, beginning with the Posebusters evaluation results presented in Table 17. Each value in the table represents the pass rate for all molecules generated by the corresponding model. For Chemical Validity and Consistency tests (including mol pred loaded, mol cond loaded, sanitization, inchi convertible, and all atoms connected), 2D models demonstrate consistently perfect performance, while 3D models show notable variations. Specifically, 3DSBDD and Pocket2Mol exhibit lower pass rates in all-atom connectivity and inchi convertibility tests. SMILES-based models show lower but consistent performance in this category, particularly in inchi convertible and all-atom connectivity metrics. Regarding Intramolecular Validity tests (covering bond lengths/angles, internal steric clash, aromatic ring flatness, double bond flatness, and internal energy), most models perform well except in the Internal Energy category. Here, significant variations are observed, with some models (3DSBDD, Pocket2Mol) showing very low pass rates while others (DST, graph-GA) achieve excellent results. For Intermolecular Validity tests (encompassing protein-ligand maximum distance, minimum distances to protein/cofactors/waters, and volume overlap with protein/cofactors/waters), nearly all models achieve perfect pass rates, with TargetDiff being the notable exception, showing poor performance in minimum distance to protein metrics. In summary, while most models excel at intermolecular validity checks, the key differences emerge in chemical validity and intramolecular metrics. 2D models maintain the most consistent performance across all categories, whereas 3D models and SMILES-based approaches display greater variability, particularly in chemical validity assessments.

We also use PoseCheck to calculate the strain energy and the steric clash of the generated poses. A clash occurs when the pairwise distance between protein and ligand atoms falls below the sum of their van der Waals radii, which is physically implausible (Ramachandran et al., 2011; Buonfiglio et al., 2015). Strain energy represents the internal energy within a ligand during binding, with lower energy typically being more favorable (Perola & Charifson, 2004).

First, we examine strain energy results in Figure 2 and Table 3, which reveal distinct patterns across model dimensions. 3D models show wide variation, with ResGen performing best (median: 12.05 kcal/mol) and TargetDiff worst (median: 487.72 kcal/mol). 2D models generally perform better, led by MolDQN (11.75 kcal/mol) and graph-GA (14.99 kcal/mol). 1D SMILES-based models show consistent performance, with SMILES-VAE (30.35 kcal/mol) outperforming others in this category.

Turning to clash results shown in Figure 4, Figure 5, Figure 6 and Table 18, we observe significant variation among 3D models. ResGen demonstrates the best performance with consistently low clash counts (median 2-4) across most receptors, while Pocket2Mol and TargetDiff exhibit high variability. In contrast, 1D and 2D models show stable performance with most models having median clash counts no higher than 10. Interestingly, receptor 8JJL consistently proves challenging for models across all categories.

In summary, while 3D models often achieve better docking scores, they do not necessarily produce better protein-ligand geometric compatibility.

4.2.3 Pharmaceutical Properties

In this section, we report and analyze the pharmaceutical properties of the generated molecules.

LogP: Overall, nearly all the models tested produced the majority of their molecules within the 0 to 3 range. For example, SMILES-LSTM-HC demonstrates remarkable consistency, maintaining a LogP score of 3.39 ± 0.60 across all targets. Several models, including Pasithea, SMILES-VAE, MIMOSA, and DST, show stable performance with LogP values between 2.40 and 2.60, indicating good potential for drug-like properties. However, there is significant variability among other models. Pocket2Mol and PocketFlow exhibit wide fluctuations in their LogP scores, ranging from -0.05 to 5.24, suggesting inconsistent control over molecular hydrophobicity. MolDQN consistently generates highly hydrophilic molecules, with LogP scores consistently below -1.0 across all targets. 3DSBDD shows the most extreme variability, with scores ranging from -11.36 to 3.73, and notably large standard deviations.

QED:Based on the results in table 13, these models demonstrate varying levels of performance across different targets. The majority of models, including SMILES-VAE, MIMOSA, and DST, consistently achieve high QED scores between 0.90-0.91, indicating their robust ability to generate drug-like molecules. A second tier of models, including SMILES-GA, SMILES-LSTM-HC, and JT-VAE, maintains reliable performance with scores ranging from 0.86 to 0.88. The graph-GA model shows moderate consistency with scores around 0.84 across all targets. Notably, there are significant performance disparities among certain models. MolDQN demonstrates considerably lower performance, with QED scores consistently falling between 0.43-0.49 across all targets. PocketFlow and 3DSBDD show variable performance, with scores fluctuating between 0.60 and 0.80, suggesting less stability in generating drug-like molecules. The performance patterns remain relatively consistent whether evaluating targets in CrossDocking or those not included in CrossDocking, indicating that the models' capabilities are generally independent of the target selection.

SA: Overall, most of the models generate molecules with scores between 1 to 3. Several models maintain consistent performance with relatively low variance: SMILES-LSTM-HC (1.93 ± 0.13), MIMOSA (1.95 ± 0.12), and DST (1.95 ± 0.14) demonstrate stable synthetic accessibility scores across all targets. However, 3DSBDD shows significantly higher scores with substantial variance, ranging from 2.89 ± 0.73 to 6.10 ± 0.96. MolDQN consistently generates molecules with higher SA scores (2.83-3.28) and notable standard deviations (0.50-0.55). The data indicates that while most models can generate synthetically accessible compounds, there are significant variations in their consistency and the complexity of the proposed synthetic routes.

Furthermore, we report the numerical values of top-K docking, QED, SA, and LogP scores for all the methods across different target proteins in the Appendix A.

4.2.4 Molecule Generation Quality

Model	Diversity	Uniqueness	Validity
SMILES-GA	0.90	0.60	1.00
SMILES-LSTM-HC	0.88	0.17	1.00
REINVENT	0.89	0.70	1.00
Pasithea	0.91	0.28	1.00
SMILES-VAE	0.88	0.54	1.00
graph-GA	0.92	0.71	1.00
MIMOSA	0.88	0.09	1.00
MolDQN	0.93	0.71	1.00
DST	0.88	0.10	1.00
JT-VAE	0.89	0.77	1.00
TargetDiff	0.89	1.00	1.00
Pocket2Mol	0.84	1.00	1.00
PocketFlow	0.89	0.84	1.00
ResGen	0.85	0.97	1.00
3DSBDD	0.89	0.80	0.80

Table 4: average Molecule Generation Metrics across all target

We record the results of Molecule Generation Oracles in Table 4 and below are the breakdown analysis.

In the diversity oracle, all models demonstrates strong capabilities with scores consistently above 0.84. MolDQN achieves the highest diversity at 0.93, followed closely by graph-GA (0.92) and Pasithea (0.91). This high-performing cluster suggests that these models are particularly adept at generating structurally varied molecules. The remaining models maintain robust diversity scores between 0.84 and 0.90, indicating generally strong performance in exploring chemical space.

In the validity oracle, nearly all models shows exceptional performance with fourteen out of fifteen models achieving perfect scores of 1. This indicates these models consistently generate chemically valid molecular structures. 3DSBDD stands as the sole exception with a validity score of 0.80, suggesting some room for improvement in ensuring chemical validity of its generated structures.

Uniqueness scores reveal the most significant variations among the three metrics. TargetDiff and Pocket2Mol achieve perfect uniqueness scores of 1.00, while ResGen (0.97) and PocketFlow (0.84) also demonstrate strong performance. However, there is a notable performance gap, with some models showing substantially lower uniqueness scores. MIMOSA (0.09), DST (0.10), and SMILES-LSTM-HC (0.17) generate relatively high proportions of duplicate structures. This variance in uniqueness scores suggests that while models can generate valid and diverse molecules, ensuring uniqueness remains a challenging aspect of molecular generation.

This comprehensive analysis indicates that while the field has largely solved the challenge of generating valid molecular structures and can consistently produce diverse molecule sets, the ability to generate unique molecules varies significantly across different approaches.

5 Discussion

Our benchmark experiments reveal a nuanced performance landscape across 1D, 2D, and 3D algorithmic families. This section provides a deeper analysis of these results, explaining the underlying reasons for the observed performance trade-offs and offering insights into the strategic application of these different approaches in drug discovery.

Intuitively, 3D models should have a decisive advantage, as they explicitly use the 3D coordinates of the target's binding pocket as input. This allows them to learn the geometric and chemical constraints imposed by the pocket's shape, directly optimizing for steric and electrostatic complementarity. Our results confirm this, showing that 3D models consistently generate molecules with superior binding affinity. However, we also observe inconsistent chemical validity and poor pose quality. There are several possible factors that can explain this "affinity-validity trade-off":

- **Sequential Error Accumulation**: Many 3D models are autoregressive, building molecules atom-by-atom. This sequential process can suffer from "exposure bias," where small geometric prediction errors in early steps accumulate, resulting in final structures with high internal strain or steric clashes, even if the overall shape fits the pocket.
- **Primacy of Coordinates over Chemistry**: The intense focus on optimizing 3D coordinates can come at the expense of enforcing fundamental, discrete rules of chemistry. This can lead to geometrically plausible but chemically unfavorable arrangements, such as strained or uncommon ring structures. Some models successfully mitigate this by explicitly incorporating chemical knowledge, like valence rules, into the generation process to improve validity.
- **Practical Hurdles**: 3D models often face practical constraints that can limit their use. They can be computationally intensive and may lack robustness, sometimes failing to generate molecules for novel protein targets without specific configurations—an issue we observed in our own experiments.

On the contrary, 1D and 2D models have better performance on chemical validity may because they are using more chemical "language" such as SMILES string or fragments and scaffolds. However these methods treat target as a "black-box oracle", generating a molecule first and only then checking its fit. This indirect optimization is inefficient for discovering high-affinity binders.

Given the complementary strengths and weaknesses of each approach, the most promising direction for future research lies in the development of hybrid models. Such framework could leverage a 1D/2D model to generate a diverse library of valid and synthesizable scaffolds, which are then passed to a 3D model for precise refinement and optimization within the target's binding pocket. This would combine the chemical robustness of 1D/2D methods with the geometric precision of 3D methods, potentially overcoming the key trade-offs identified in this benchmark.

6 Conclusion

Currently, the landscape of structure-based drug design models is vast, featuring various algorithmic backbones, yet comparative analyses across them are scarce. In this study, we design experiments to evaluate the quality of molecules generated by each model. Our experiments extend beyond conventional heuristic oracles related to molecular properties, also examining the affinity and poses between molecules and selected target proteins. Our findings indicate that different algorithmic approaches exhibit distinct strengths and limitations. 3D models, particularly Pocket2Mol, demonstrate superior performance in generating molecules with strong binding affinities, as evidenced by docking scores. However, they show more variability in chemical validity checks and pose evaluations. 1D SMILES-based models maintain consistent performance across most metrics but rarely achieve the highest binding affinities. 2D graph-based models offer the most balanced performance, showing strong consistency across chemical validity, pose quality, and moderate binding affinity scores.

These results suggest that while significant progress has been made in structure-based drug design, there remains room for improvement in developing models that can simultaneously optimize binding affinity while maintaining high chemical validity and pose quality. Future development of structure-based models should focus on bridging these gaps, potentially by incorporating mechanisms that better balance the trade-offs between binding affinity optimization and other crucial molecular properties. This comprehensive evaluation provides valuable insights for researchers working to advance the field of computational drug discovery.

References

Mostapha Benhenda. Chemgan challenge for drug discovery: can ai reproduce natural chemical diversity?, 2017.

Tom L Blundell. Structure-based drug design. *Nature*, 384(6604):23, 1996.

Regine S Bohacek, Colin McMartin, and Wayne C Guida. The art and practice of structure-based drug design: a molecular modeling perspective. *Medicinal research reviews*, 16(1):3–50, 1996.

Nathan Brown, Marco Fiscato, Marwin H.S. Segler, and Alain C. Vaucher. Guacamol: Benchmarking models for de novo molecular design. *Journal of Chemical Information and Modeling*, 59(3):1096–1108, March 2019. ISSN 1549-960X. doi: 10.1021/acs.jcim.8b00839. URL http://dx.doi.org/10.1021/acs.jcim.8b00839.

Rosa Buonfiglio, Maurizio Recanatini, and Matteo Masetti. Protein flexibility in drug discovery: From theory to computation. *ChemMedChem*, 10(7):1141–1148, 2015. doi: https://doi.org/10.1002/cmdc.201500086. URL https://chemistry-europe.onlinelibrary.wiley.com/doi/abs/10.1002/cmdc.201500086.

Martin Buttenschoen, Garrett M. Morris, and Charlotte M. Deane. Posebusters: Ai-based docking methods fail to generate physically valid poses or generalise to novel sequences. *Chemical Science*, 15(9):3130–3139, 2024. ISSN 2041-6539. doi: 10.1039/d3sc04185a. URL http://dx.doi.org/10.1039/D3SC04185A.

Yi-Tan Chang, Eric P Hoffman, Guoqiang Yu, David M Herrington, Robert Clarke, Chiung-Ting Wu, Lulu Chen, and Yue Wang. Integrated identification of disease specific pathways using multi-omics data. *bioRxiv*, pp. 666065, 2019.

Yuanqi Du, Tianfan Fu, Jimeng Sun, and Shengchao Liu. Molgensurvey: A systematic survey in machine learning models for molecule design. *arXiv preprint arXiv:2203.14500*, 2022.

Jerome Eberhardt, Diogo Santos-Martins, Andreas F. Tillack, and Stefano Forli. Autodock vina 1.2.0: New docking methods, expanded force field, and python bindings. *Journal of Chemical Information and Modeling*, 61(8):3891–3898, 2021. doi: 10.1021/acs.jcim.1c00203. URL https://doi.org/10.1021/acs.jcim.1c00203. PMID: 34278794.

Paul G Francoeur, Tomohide Masuda, Jocelyn Sunseri, Andrew Jia, Richard B Iovanisci, Ian Snyder, and David R Koes. Three-dimensional convolutional neural networks and a cross-docked data set for structure-based drug design. *Journal of chemical information and modeling*, 60(9):4200–4215, 2020.

Tianfan Fu, Cao Xiao, Xinhao Li, Lucas M Glass, and Jimeng Sun. Mimosa: Multi-constraint molecule sampling for molecule optimization. In *Proceedings of the AAAI Conference on Artificial Intelligence*, volume 35, pp. 125–133, 2021.

Tianfan Fu, Wenhao Gao, Connor W. Coley, and Jimeng Sun. Reinforced genetic algorithm for structure-based drug design, 2022a.

Tianfan Fu, Wenhao Gao, Cao Xiao, Jacob Yasonik, Connor W. Coley, and Jimeng Sun. Differentiable scaffolding tree for molecular optimization, 2022b.

Wenhao Gao, Tianfan Fu, Jimeng Sun, and Connor W. Coley. Sample efficiency matters: A benchmark for practical molecular optimization, 2022.

David E. Graff, Eugene I. Shakhnovich, and Connor W. Coley. Accelerating high-throughput virtual screening through molecular pool-based active learning. *Chemical Science*, 12(22):7866–7881, 2021. ISSN 2041-6539. doi: 10.1039/d0sc06805e. URL http://dx.doi.org/10.1039/d0sc06805e.

Jiaqi Guan, Wesley Wei Qian, Xingang Peng, Yufeng Su, Jian Peng, and Jianzhu Ma. 3d equivariant diffusion for target-aware molecule generation and affinity prediction. In *International Conference on Learning Representations*, 2023.

Rafael Gómez-Bombarelli, Jennifer N. Wei, David Duvenaud, José Miguel Hernández-Lobato, Benjamín Sánchez-Lengeling, Dennis Sheberla, Jorge Aguilera-Iparraguirre, Timothy D. Hirzel, Ryan P. Adams, and Alán Aspuru-Guzik. Automatic chemical design using a data-driven continuous representation of molecules. *ACS Central Science*, 4(2):268–276, January 2018. ISSN 2374-7951. doi: 10.1021/acscentsci.7b00572. URL http://dx.doi.org/10.1021/acscentsci.7b00572.

Charles Harris, Kieran Didi, Arian R Jamasb, Chaitanya K Joshi, Simon V Mathis, Pietro Lio, and Tom Blundell. Benchmarking generated poses: How rational is structure-based drug design with generative models? *arXiv preprint arXiv:2308.07413*, 2023.

Bahareh Honarparvar, Thavendran Govender, Glenn EM Maguire, Mahmoud ES Soliman, and Hendrik G Kruger. Integrated approach to structure-based enzymatic drug design: molecular modeling, spectroscopy, and experimental bioactivity. *Chemical reviews*, 114(1):493–537, 2014.

Kexin Huang, Tianfan Fu, Wenhao Gao, Yue Zhao, Yusuf Roohani, Jure Leskovec, Connor W Coley, Cao Xiao, Jimeng Sun, and Marinka Zitnik. Therapeutics data commons: Machine learning datasets and tasks for drug discovery and development. *arXiv preprint arXiv:2102.09548*, 2021.

Kexin Huang, Tianfan Fu, Wenhao Gao, Yue Zhao, Yusuf Roohani, Jure Leskovec, Connor W Coley, Cao Xiao, Jimeng Sun, and Marinka Zitnik. Artificial intelligence foundation for therapeutic science. *Nature Chemical Biology*, 2022.

Jan H Jensen. A graph-based genetic algorithm and generative model/monte carlo tree search for the exploration of chemical space. *Chemical science*, 10(12):3567–3572, 2019.

Yuanyuan Jiang, Guo Zhang, Jing You, Hailin Zhang, Rui Yao, Huanzhang Xie, Liyun Zhang, Ziyi Xia, Mengzhe Dai, Yunjie Wu, Linli Li, and Shengyong Yang. Pocketflow is a data-and-knowledge-driven structure-based molecular generative model. *Nature Machine Intelligence*, 6:1–12, 03 2024. doi: 10.1038/s42256-024-00808-8.

Wengong Jin, Regina Barzilay, and Tommi Jaakkola. Junction tree variational autoencoder for molecular graph generation, 2019. URL https://arxiv.org/abs/1802.04364.

Haoyang Liu, Yifei Qin, Zhangming Niu, Mingyuan Xu, Jiaqiang Wu, Xianglu Xiao, Jinping Lei, Ting Ran, and Hongming Chen. How good are current pocket-based 3d generative models?: The benchmark set and evaluation of protein pocket-based 3d molecular generative models. *Journal of Chemical Information and Modeling*, 64(24):9260–9275, 2024. doi: 10.1021/acs.jcim.4c01598. URL https://doi.org/10.1021/acs.jcim.4c01598. PMID: 39629985.

Alston Lo, Robert Pollice, AkshatKumar Nigam, Andrew D. White, Mario Krenn, and Alán Aspuru-Guzik. Recent advances in the self-referencing embedded strings (selfies) library, 2023. URL http://dx.doi.org/10.1039/D3DD00044C.

Yingzhou Lu, Chiung-Ting Wu, Sarah J Parker, Zuolin Cheng, Georgia Saylor, Jennifer E Van Eyk, Guoqiang Yu, Robert Clarke, David M Herrington, and Yue Wang. Cot: an efficient and accurate method for detecting marker genes among many subtypes. *Bioinformatics Advances*, 2(1):vbac037, 2022.

Shitong Luo, Jiaqi Guan, Jianzhu Ma, and Jian Peng. A 3d generative model for structure-based drug design. In *Thirty-Fifth Conference on Neural Information Processing Systems*, 2021.

Marcus Olivecrona, Thomas Blaschke, Ola Engkvist, and Hongming Chen. Molecular de novo design through deep reinforcement learning. *Journal of Cheminformatics*, 9, 09 2017. doi: 10.1186/s13321-017-0235-x.

Xingang Peng, Shitong Luo, Jiaqi Guan, Qi Xie, Jian Peng, and Jianzhu Ma. Pocket2mol: Efficient molecular sampling based on 3d protein pockets, 2022.

Emanuele Perola and Paul S. Charifson. Conformational analysis of drug-like molecules bound to proteins: An extensive study of ligand reorganization upon binding. *Journal of Medicinal Chemistry*, 47(10):2499–2510, 2004. doi: 10.1021/jm030563w. URL https://doi.org/10.1021/jm030563w. PMID: 15115393.

Daniil Polykovskiy, Alexander Zhebrak, Benjamin Sanchez-Lengeling, Sergey Golovanov, Oktai Tatanov, Stanislav Belyaev, Rauf Kurbanov, Aleksey Artamonov, Vladimir Aladinskiy, Mark Veselov, Artur Kadurin, Simon Johansson, Hongming Chen, Sergey Nikolenko, Alán Aspuru-Guzik, and Alex Zhavoronkov. Molecular sets (moses): A benchmarking platform for molecular generation models. *Frontiers in Pharmacology*, 11, 2020. ISSN 1663-9812. doi: 10.3389/fphar.2020.565644. URL https://www.frontiersin.org/articles/10.3389/fphar.2020.565644.

Srinivas Ramachandran, Pradeep Kota, Feng Ding, and Nikolay V. Dokholyan. Automated minimization of steric clashes in protein structures. *Proteins: Structure, Function, and Bioinformatics*, 79(1):261–270, 2011. doi: https://doi.org/10.1002/prot.22879. URL https://onlinelibrary.wiley.com/doi/abs/10.1002/prot.22879.

Bart Selman and Carla P Gomes. Hill-climbing search. *Encyclopedia of cognitive science*, 81:82, 2006.

Cynthia Shen, Mario Krenn, Sagi Eppel, and Alán Aspuru-Guzik. Deep molecular dreaming: inverse machine learning for de-novo molecular design and interpretability with surjective representations. *Machine Learning: Science and Technology*, 2(3):03LT02, July 2021. ISSN 2632-2153. doi: 10.1088/2632-2153/ac09d6. URL http://dx.doi.org/10.1088/2632-2153/ac09d6.

Sandeep Sinha and Divya Vohora. Drug discovery and development: An overview. *Pharmaceutical medicine and translational clinical research*, pp. 19–32, 2018.

Jacob O. Spiegel and Jacob D. Durrant. Autogrow4: an open-source genetic algorithm for de novo drug design and lead optimization. *Journal of Cheminformatics*, 12(1):25, 2020. ISSN 1758-2946. doi: 10.1186/s13321-020-00429-4. URL https://doi.org/10.1186/s13321-020-00429-4.

Ashutosh Tripathi and Vytas A Bankaitis. Molecular docking: From lock and key to combination lock. *Journal of molecular medicine and clinical applications*, 2(1), 2017.

Austin Tripp and José Miguel Hernández-Lobato. Genetic algorithms are strong baselines for molecule generation, 2023.

Austin Tripp, Gregor NC Simm, and José Miguel Hernández-Lobato. A fresh look at de novo molecular design benchmarks. In *NeurIPS 2021 AI for Science Workshop*, 2021.

David Weininger. Smiles, a chemical language and information system. 1. introduction to methodology and encoding rules. *Journal of Chemical Information and Computer Sciences*, 28(1):31–36, 1988. doi: 10.1021/ci00057a005. URL https://doi.org/10.1021/ci00057a005.

Naruki Yoshikawa, Kei Terayama, Masato Sumita, Teruki Homma, Kenta Oono, and Koji Tsuda. Population-based De Novo Molecule Generation, Using Grammatical Evolution. *Chemistry Letters*, 47(11):1431–1434, 10 2018. ISSN 0366-7022. doi: 10.1246/cl.180665. URL https://doi.org/10.1246/cl.180665.

Odin Zhang, Jintu Zhang, Jieyu Jin, Xujun Zhang, RenLing Hu, Chao Shen, Hanqun Cao, Hongyan Du, Yu Kang, Yafeng Deng, Furui Liu, Guangyong Chen, Chang-Yu Hsieh, and Tingjun Hou. Resgen is a pocket-aware 3d molecular generation model based on parallel multiscale modelling. *Nature Machine Intelligence*, 5(9):1020–1030, September 2023. ISSN 2522-5839. doi: 10.1038/s42256-023-00712-7. URL https://doi.org/10.1038/s42256-023-00712-7.

Zhenpeng Zhou, Steven Kearnes, Li Li, Richard N. Zare, and Patrick Riley. Optimization of molecules via deep reinforcement learning. *Scientific Reports*, 9(1):10752, 2019. ISSN 2045-2322. doi: 10.1038/s41598-019-47148-x. URL https://doi.org/10.1038/s41598-019-47148-x.

A Appendix

Table 5: Number of successfully generated and stored molecules by model. Targets in CrossDocking are marked in red, and targets not in CrossDocking are in blue.

Model	6GL8	1UWH	7OTE	1KKQ	5WFD	7WC7	8JJL	7D42	6AZV	7S1S
SMILES-GA	832	800	819	892	580	791	652	662	629	558
SMILES-LSTM-HC	1000	1000	1000	1000	1000	1000	1000	1000	1000	1000
REINVENT	1000	1000	1000	1000	1000	1000	1000	1000	1000	1000
Pasithea	1000	800	900	1000	1000	800	900	800	1000	1000
SMILES-VAE	1000	1000	1000	600	1000	1000	1000	1000	1000	1000
graph GA	1000	1000	400	1000	1000	1000	500	1000	1000	1000
MIMOSA	1000	1000	1000	1000	1000	1000	1000	1000	1000	1000
MolDQN	700	690	700	800	700	700	700	700	700	696
DST	1000	900	1000	1000	1000	1000	900	1000	1000	1000
JT-VAE	1000	1000	1000	1000	1000	200	1000	1000	1000	1000
TargetDiff	0	1	0	557	70	4	10	1	0	0
3DSBDD	898	708	669	668	769	1000	1000	1000	222	673
Pocket2mol	1000	968	1000	790	1000	1000	860	884	868	1000
PocketFlow	1000	1000	1000	1000	1000	1000	1000	1000	1000	1000
ResGen	0	676	290	785	0	259	0	805	1000	1000

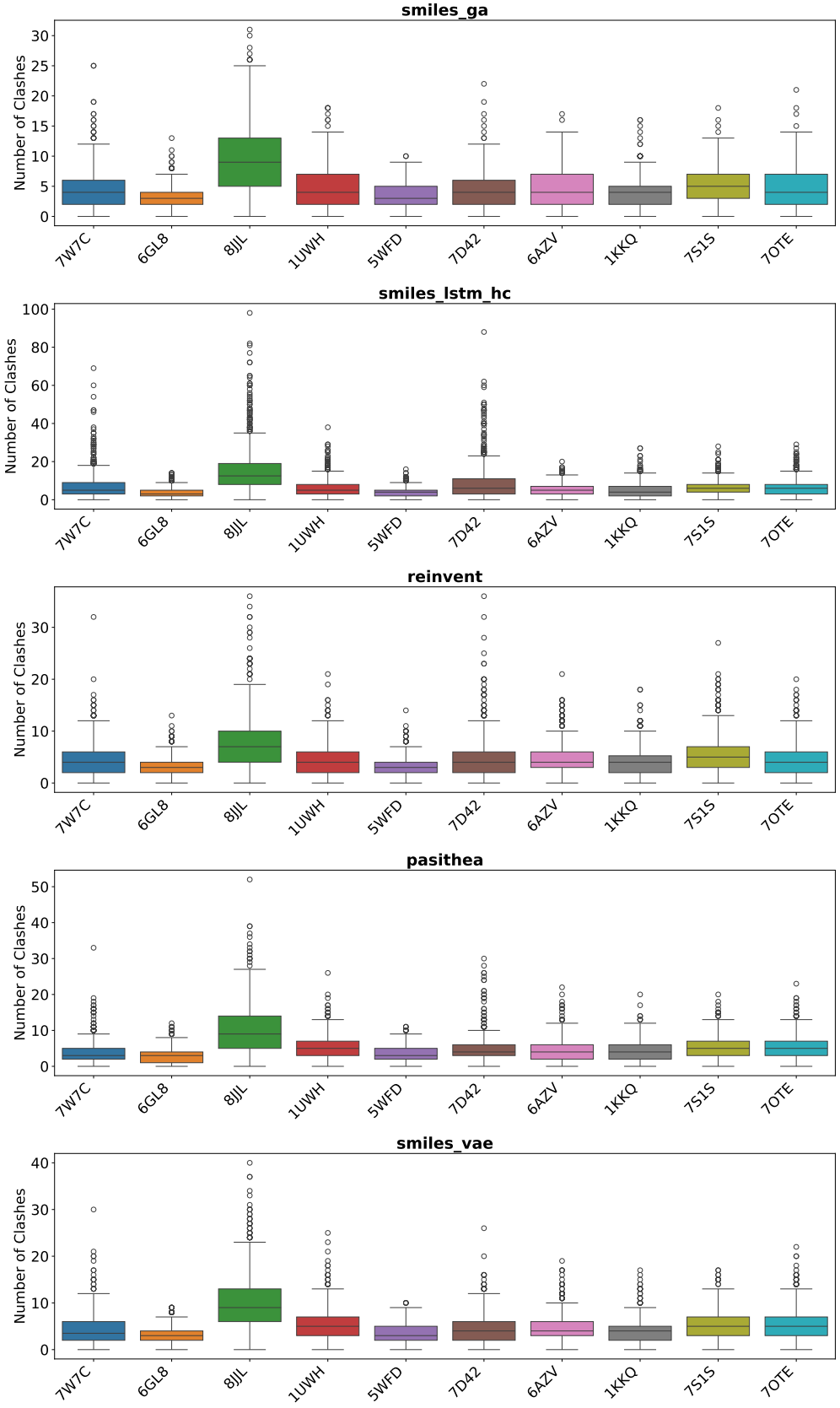

Figure 4: The clashes box plot for 1D models

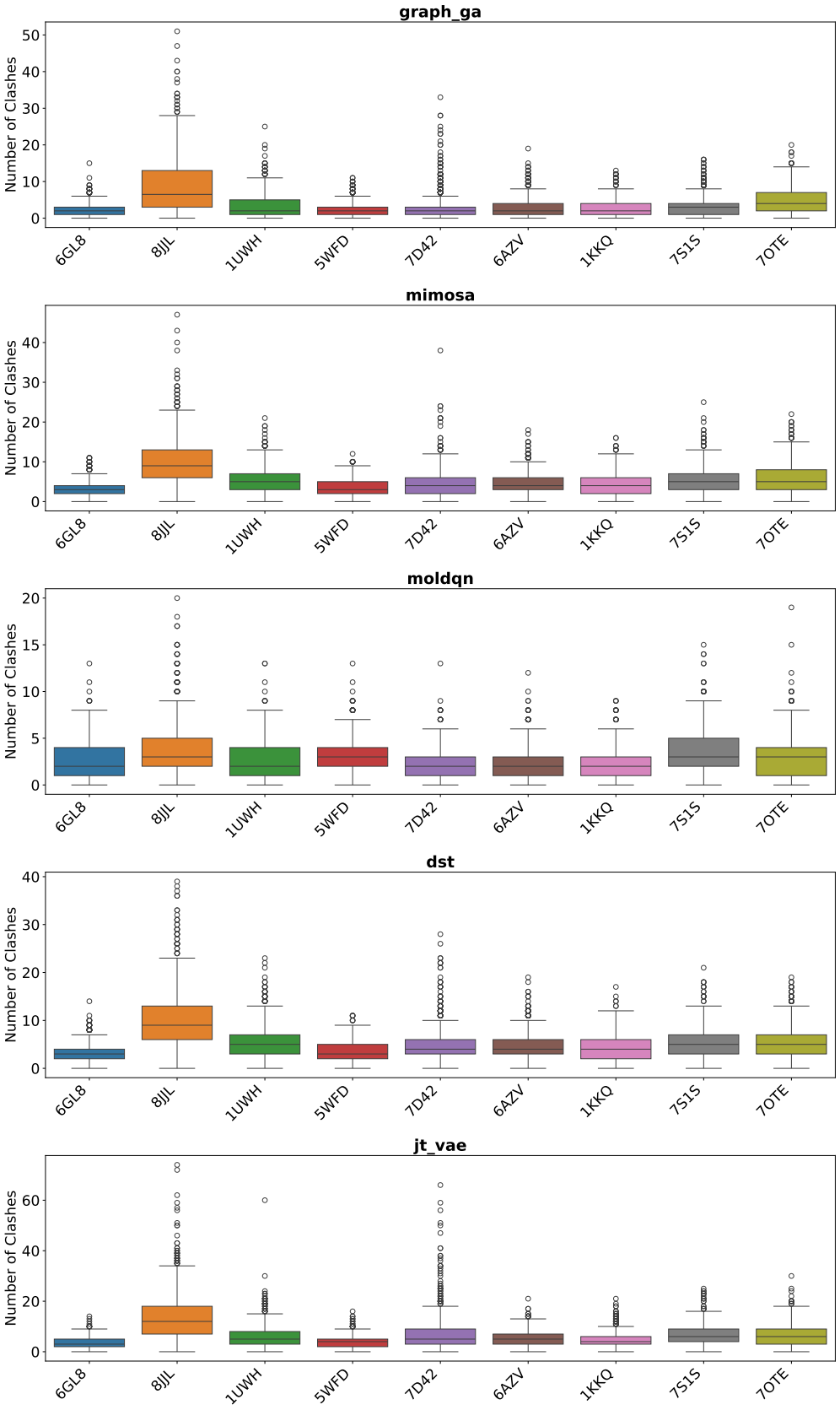

Figure 5: The clashes box plot for 2D models

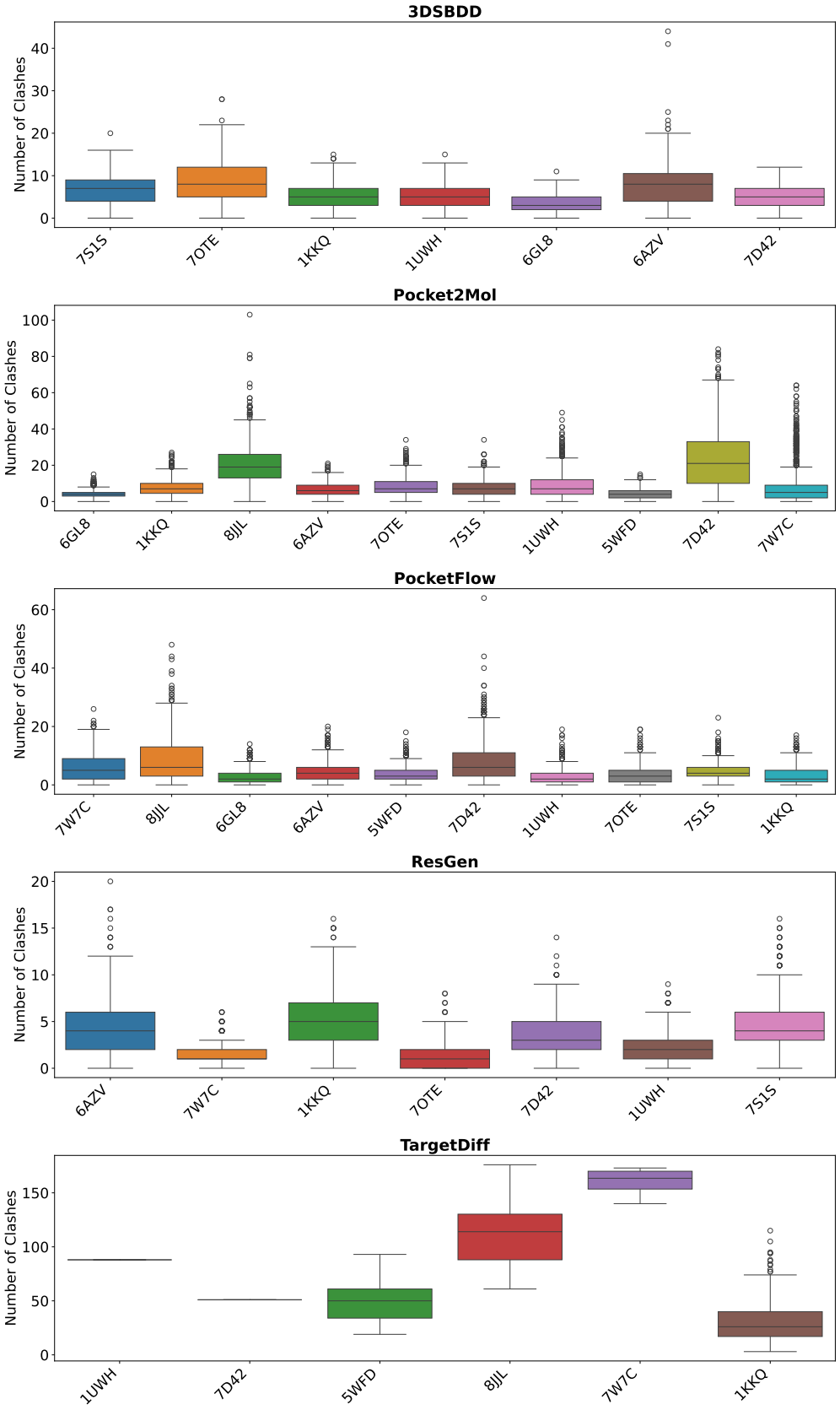

Figure 6: The clashes box plot for 3D models

Model	6GL8	1UWH	7OTE	1KKQ	5WFD
Pocket2Mol	**-10.53** ± 0.40	**-13.87** ± 0.34	**-14.78** ± 0.44	**-13.53** ± 0.30	**-11.06** ± 0.15
PocketFlow	-8.98 ± 0.22	-10.68 ± 0.23	-9.55 ± 0.36	-11.67 ± 0.38	-9.34 ± 0.35
ResGen	–	-9.23 ± 0.20	-7.03 ± 0.06	-9.56 ± 0.18	–
3DSBDD	-8.19 ± 0.22	-12.41 ± 0.18	-10.41 ± 0.09	-12.71 ± 0.30	-10.72 ± 0.22
DST	-8.23 ± 0.15	-10.48 ± 0.16	-10.76 ± 0.21	-9.96 ± 0.32	-9.22 ± 0.28
graph-GA	-7.94 ± 0.18	-10.12 ± 0.37	-9.94 ± 0.36	-9.63 ± 0.32	-9.03 ± 0.18
JT-VAE	-9.09 ± 0.42	-11.12 ± 0.41	-11.27 ± 0.34	-10.90 ± 0.47	-10.26 ± 0.42
MIMOSA	-8.28 ± 0.13	-10.52 ± 0.22	-10.82 ± 0.25	-10.16 ± 0.25	-9.35 ± 0.19
MolDQN	-6.13 ± 0.17	-6.69 ± 0.25	-6.93 ± 0.20	-6.75 ± 0.21	-7.37 ± 0.14
Pasithea	-8.73 ± 0.24	-11.12 ± 0.27	-10.84 ± 0.26	-10.13 ± 0.18	-9.88 ± 0.33
REINVENT	-8.65 ± 0.24	-10.72 ± 0.28	-10.76 ± 0.44	-10.51 ± 0.28	-9.56 ± 0.24
SMILES-GA	-8.44 ± 0.23	-10.33 ± 0.27	-10.27 ± 0.39	-9.81 ± 0.38	-9.20 ± 0.30
SMILES-LSTM-HC	-9.26 ± 0.29	-11.02 ± 0.25	-11.54 ± 0.40	-11.21 ± 0.51	-10.41 ± 0.42
SMILES-VAE	-8.76 ± 0.25	-11.13 ± 0.37	-11.35 ± 0.61	-10.31 ± 0.31	-9.74 ± 0.16
TargetDiff	–	–	–	-11.14 ± 0.26	-8.29 ± 0.69

(a) Targets in CrossDocking.

Model	7W7C	8JJL	7D42	7S1S	6AZV
Pocket2Mol	**-13.56** ± 0.11	**-12.79** ± 0.33	-12.10 ± 0.33	**-12.49** ± 0.26	**-11.87** ± 0.26
PocketFlow	-13.02 ± 0.23	-11.42 ± 0.28	**-12.25** ± 0.30	-9.46 ± 0.34	-11.49 ± 0.15
ResGen	-7.56 ± 0.18	–	-8.60 ± 0.20	-11.63 ± 0.08	-9.47 ± 0.13
3DSBDD	-10.78 ± 0.28	-10.90 ± 0.35	-10.43 ± 0.29	-9.84 ± 0.21	-9.66 ± 0.32
DST	-11.11 ± 0.37	-10.79 ± 0.48	-10.92 ± 0.32	-10.73 ± 0.30	-9.78 ± 0.16
graph-GA	-10.60 ± 0.39	-10.23 ± 0.19	-10.43 ± 0.20	-9.98 ± 0.16	-9.14 ± 0.21
JT-VAE	-10.81 ± 0.54	-10.81 ± 0.39	-11.52 ± 0.41	-11.04 ± 0.16	-10.18 ± 0.14
MIMOSA	-11.14 ± 0.21	-10.77 ± 0.36	-11.03 ± 0.29	-10.78 ± 0.33	-9.78 ± 0.18
MolDQN	-7.33 ± 0.16	-7.90 ± 0.35	-6.53 ± 0.26	-8.01 ± 0.16	-6.73 ± 0.39
Pasithea	-11.41 ± 0.26	-11.24 ± 0.32	-11.15 ± 0.26	-11.06 ± 0.18	-10.03 ± 0.12
REINVENT	-11.52 ± 0.19	-11.13 ± 0.25	-11.40 ± 0.34	-10.99 ± 0.20	-9.92 ± 0.30
SMILES-GA	-10.97 ± 0.29	-11.01 ± 0.18	-11.01 ± 0.43	-10.46 ± 0.35	-9.41 ± 0.40
SMILES-LSTM-HC	-12.20 ± 0.60	-11.09 ± 0.18	-11.47 ± 0.46	-11.47 ± 0.24	-10.38 ± 0.13
SMILES-VAE	-11.42 ± 0.33	-11.14 ± 0.42	-11.42 ± 0.27	-11.14 ± 0.34	-10.11 ± 0.19
TargetDiff	–	-7.99 ± 0.53	–	–	–

(b) Targets not in CrossDocking.

Table 6: Top 10 Vina score for each target.

Model	6GL8	1UWH	7OTE	1KKQ	5WFD
Pocket2Mol	-9.90 ± 0.31	-12.81 ± 0.48	-13.14 ± 0.78	-12.36 ± 0.52	-10.45 ± 0.29
PocketFlow	-7.92 ± 0.52	-8.12 ± 1.43	-7.74 ± 0.85	-10.33 ± 0.60	-8.14 ± 0.56
ResGen	–	-8.06 ± 0.56	-6.30 ± 0.48	-8.82 ± 0.35	–
3DSBDD	-7.22 ± 0.44	-11.52 ± 0.44	-9.67 ± 0.38	-11.59 ± 0.51	-9.86 ± 0.40
DST	-7.50 ± 0.28	-9.41 ± 0.40	-9.47 ± 0.49	-9.00 ± 0.40	-8.41 ± 0.31
graph-GA	-6.81 ± 0.40	-8.32 ± 0.68	-8.25 ± 0.65	-8.07 ± 0.59	-7.65 ± 0.49
JT-VAE	-7.93 ± 0.48	-9.82 ± 0.51	-9.65 ± 0.59	-9.62 ± 0.53	-9.00 ± 0.48
MIMOSA	-7.49 ± 0.27	-9.54 ± 0.38	-9.49 ± 0.48	-8.99 ± 0.40	-8.46 ± 0.32
MolDQN	-4.84 ± 0.47	-5.46 ± 0.47	-5.87 ± 0.40	-5.65 ± 0.43	-5.79 ± 0.56
Pasithea	-7.93 ± 0.39	-9.94 ± 0.51	-9.98 ± 0.43	-9.36 ± 0.36	-8.92 ± 0.44
REINVENT	-7.82 ± 0.36	-9.70 ± 0.43	-9.77 ± 0.48	-9.40 ± 0.51	-8.80 ± 0.36
SMILES-GA	-7.37 ± 0.46	-8.94 ± 0.66	-8.95 ± 0.64	-8.64 ± 0.50	-8.12 ± 0.44
SMILES-LSTM-HC	-8.29 ± 0.42	-10.18 ± 0.41	-10.40 ± 0.50	-10.10 ± 0.49	-9.43 ± 0.43
SMILES-VAE	-7.97 ± 0.37	-9.97 ± 0.50	-10.09 ± 0.56	-9.08 ± 0.52	-8.84 ± 0.40
TargetDiff	–	–	–	-9.84 ± 0.58	–

a): targets in CrossDocking

Model	7W7C	8JJL	7D42	7S1S	6AZV
Pocket2Mol	-12.55 ± 0.49	-11.63 ± 0.51	-10.88 ± 0.56	-11.51 ± 0.46	-11.11 ± 0.36
PocketFlow	-11.94 ± 0.47	-10.35 ± 0.46	-11.11 ± 0.48	-7.82 ± 0.74	-10.56 ± 0.40
ResGen	-7.04 ± 0.24	–	-7.71 ± 0.44	-11.06 ± 0.31	-8.75 ± 0.32
3DSBDD	-8.67 ± 1.14	-9.58 ± 0.57	-9.10 ± 0.64	-8.95 ± 0.42	-8.28 ± 0.64
DST	-10.06 ± 0.41	-9.74 ± 0.45	-9.92 ± 0.41	-9.78 ± 0.37	-8.90 ± 0.30
graph-GA	-8.89 ± 0.64	-8.52 ± 0.61	-8.82 ± 0.57	-8.46 ± 0.52	-7.88 ± 0.48
JT-VAE	-8.63 ± 0.79	-9.78 ± 0.43	-10.30 ± 0.48	-10.07 ± 0.35	-9.02 ± 0.42
MIMOSA	-10.08 ± 0.40	-9.74 ± 0.45	-9.88 ± 0.45	-9.77 ± 0.41	-8.85 ± 0.34
MolDQN	-6.12 ± 0.43	-6.57 ± 0.53	-5.41 ± 0.42	-6.38 ± 0.53	-5.78 ± 0.38
Pasithea	-10.53 ± 0.42	-10.22 ± 0.45	-10.31 ± 0.40	-10.23 ± 0.42	-9.30 ± 0.35
REINVENT	-10.46 ± 0.48	-10.26 ± 0.41	-10.32 ± 0.48	-10.08 ± 0.41	-9.19 ± 0.34
SMILES-GA	-9.78 ± 0.55	-9.61 ± 0.62	-9.39 ± 0.66	-9.30 ± 0.50	-8.50 ± 0.43
SMILES-LSTM-HC	-11.09 ± 0.50	-10.16 ± 0.43	-10.62 ± 0.43	-10.51 ± 0.44	-9.52 ± 0.37
SMILES-VAE	-10.54 ± 0.42	-10.17 ± 0.45	-10.34 ± 0.51	-10.22 ± 0.44	-9.32 ± 0.36
TargetDiff	–	–	–	–	–

b): targets not in CrossDocking

Table 7: Top 100 Average docking score for each target

Table 8: Top 1 LogP score for each target. Targets in CrossDocking are marked in red, and targets not in CrossDocking are in blue.

Model	6GL8	1UWH	7OTE	1KKQ	5WFD	7W7C	8JJL	7D42	7S1S	6AZV
SMILES-GA	3.59	3.59	3.59	3.59	3.59	3.59	3.59	3.59	3.59	3.59
SMILES-LSTM-HC	6.88	5.60	6.88	6.88	6.88	6.88	6.88	6.88	6.88	6.88
REINVENT	3.55	3.85	3.85	3.73	3.39	3.39	3.39	3.39	4.04	3.39
Pasithea	3.35	3.48	3.24	3.38	3.24	3.24	3.24	3.24	3.24	3.24
SMILES-VAE	3.55	3.82	3.87	3.84	3.86	3.55	3.73	3.56	3.63	4.20
graph-GA	3.59	3.59	3.66	4.19	3.96	3.78	3.59	3.81	3.59	3.59
MIMOSA	4.15	4.15	4.15	4.15	4.15	4.15	4.15	4.15	4.15	4.15
MolDQN	0.49	1.00	1.07	1.07	0.56	1.00	1.00	0.29	1.00	1.45
DST	3.44	3.31	3.44	3.44	3.44	3.44	3.31	3.44	3.44	3.44
JT-VAE	3.93	3.91	3.91	4.37	4.70	3.75	4.10	3.75	3.75	4.36
TargetDiff	–	-0.67	–	4.43	1.30	3.08	0.15	-0.28	–	–
Pocket2Mol	5.49	3.72	5.23	6.31	4.22	3.30	4.27	4.04	3.27	5.04
PocketFlow	4.92	3.94	3.86	6.76	4.89	6.19	4.87	5.80	3.04	6.85
ResGen	–	3.29	2.18	3.75	–	2.90	–	2.90	2.79	2.90
3DSBDD	2.41	3.51	0.72	3.30	1.23	2.01	6.93	3.79	1.14	2.67

Model	6GL8	1UWH	7OTE	1KKQ	5WFD
SMILES-GA	2.58 ± 0.44	2.55 ± 0.42	2.53 ± 0.44	2.43 ± 0.51	2.57 ± 0.43
SMILES-LSTM-HC	4.64 ± 1.03	4.52 ± 0.41	4.64 ± 1.03	4.64 ± 1.03	4.64 ± 1.03
REINVENT	3.14 ± 0.25	3.22 ± 0.27	3.13 ± 0.33	3.12 ± 0.29	3.02 ± 0.23
Pasithea	3.08 ± 0.12	3.04 ± 0.18	3.06 ± 0.09	3.06 ± 0.16	3.06 ± 0.09
SMILES-VAE	3.33 ± 0.09	3.36 ± 0.18	3.33 ± 0.26	3.34 ± 0.20	3.47 ± 0.19
graph-GA	2.78 ± 0.33	3.04 ± 0.32	3.00 ± 0.34	3.29 ± 0.51	3.20 ± 0.32
MIMOSA	3.34 ± 0.28	3.34 ± 0.28	3.34 ± 0.28	3.34 ± 0.28	3.34 ± 0.28
MolDQN	0.27 ± 0.20	-0.13 ± 0.49	0.27 ± 0.49	0.50 ± 0.31	0.02 ± 0.32
DST	3.14 ± 0.14	3.09 ± 0.11	3.14 ± 0.14	3.14 ± 0.14	3.14 ± 0.14
JT-VAE	3.45 ± 0.28	3.54 ± 0.24	3.51 ± 0.20	3.71 ± 0.29	3.87 ± 0.46
TargetDiff	–	-0.67 ± 0.00	–	3.79 ± 0.36	-0.11 ± 0.87
Pocket2Mol	5.00 ± 0.21	3.33 ± 0.18	4.93 ± 0.18	6.00 ± 0.15	3.88 ± 0.21
PocketFlow	4.35 ± 0.27	2.29 ± 0.73	3.01 ± 0.58	6.03 ± 0.40	3.78 ± 0.49
ResGen	–	2.83 ± 0.18	1.78 ± 0.22	3.58 ± 0.08	–
3DSBDD	1.98 ± 0.23	2.72 ± 0.47	-0.59 ± 0.49	2.93 ± 0.24	0.33 ± 0.56

a): targets in CrossDocking

Model	7W7C	8JJL	7D42	7S1S	6AZV
SMILES-GA	2.55 ± 0.50	2.84 ± 0.28	2.59 ± 0.43	2.45 ± 0.49	2.54 ± 0.45
SMILES-LSTM-HC	4.64 ± 1.03	4.64 ± 1.03	4.64 ± 1.03	4.64 ± 1.03	4.64 ± 1.03
REINVENT	3.07 ± 0.22	3.13 ± 0.18	3.02 ± 0.23	3.38 ± 0.37	3.07 ± 0.21
Pasithea	3.06 ± 0.09	3.06 ± 0.09	3.06 ± 0.09	3.06 ± 0.09	3.06 ± 0.09
SMILES-VAE	3.31 ± 0.10	3.38 ± 0.15	3.35 ± 0.13	3.37 ± 0.17	3.32 ± 0.30
graph-GA	3.07 ± 0.39	2.92 ± 0.34	3.00 ± 0.40	3.03 ± 0.27	2.80 ± 0.29
MIMOSA	3.34 ± 0.28	3.34 ± 0.28	3.34 ± 0.28	3.34 ± 0.28	3.34 ± 0.28
MolDQN	0.15 ± 0.38	-0.09 ± 0.54	-0.23 ± 0.34	0.04 ± 0.36	0.06 ± 0.65
DST	3.14 ± 0.14	3.09 ± 0.11	3.14 ± 0.14	3.14 ± 0.14	3.14 ± 0.14
JT-VAE	2.94 ± 0.36	3.47 ± 0.34	3.38 ± 0.16	3.37 ± 0.18	3.58 ± 0.41
TargetDiff	1.01 ± 1.35	-7.95 ± 20.45	-0.28 ± 0.00	–	–
Pocket2Mol	2.78 ± 0.29	3.98 ± 0.13	3.54 ± 0.27	2.74 ± 0.23	4.38 ± 0.32
PocketFlow	5.50 ± 0.36	3.84 ± 0.51	5.48 ± 0.21	1.15 ± 0.79	6.40 ± 0.26
ResGen	2.59 ± 0.16	–	2.48 ± 0.19	2.36 ± 0.15	2.58 ± 0.20
3DSBDD	0.91 ± 0.60	6.19 ± 0.35	2.94 ± 0.43	-0.19 ± 0.64	1.71 ± 0.41

b): targets not in CrossDocking

Table 9: Top 10 LogP score for each target

Model	6GL8	1UWH	7OTE	1KKQ	5WFD
SMILES-GA	1.25 ± 0.62	1.36 ± 0.57	1.24 ± 0.63	0.93 ± 0.75	1.32 ± 0.63
SMILES-LSTM-HC	3.39 ± 0.60	3.38 ± 0.55	3.39 ± 0.60	3.39 ± 0.60	3.39 ± 0.60
REINVENT	2.21 ± 0.47	2.11 ± 0.58	2.12 ± 0.51	2.11 ± 0.53	2.08 ± 0.49
Pasithea	2.44 ± 0.35	2.40 ± 0.31	2.50 ± 0.30	2.42 ± 0.32	2.50 ± 0.30
SMILES-VAE	2.56 ± 0.40	2.55 ± 0.38	2.57 ± 0.34	2.45 ± 0.44	2.58 ± 0.42
graph-GA	1.61 ± 0.61	1.81 ± 0.58	1.64 ± 0.64	1.89 ± 0.65	1.99 ± 0.57
MIMOSA	2.55 ± 0.38	2.55 ± 0.38	2.55 ± 0.38	2.55 ± 0.38	2.55 ± 0.38
MolDQN	-1.41 ± 0.72	-1.67 ± 0.66	-1.51 ± 0.75	-1.17 ± 0.76	-1.62 ± 0.71
DST	2.60 ± 0.28	2.57 ± 0.27	2.60 ± 0.28	2.60 ± 0.28	2.60 ± 0.28
JT-VAE	2.25 ± 0.54	2.54 ± 0.49	2.52 ± 0.47	2.47 ± 0.56	2.46 ± 0.63
TargetDiff	–	-0.67 ± 0.00	–	2.14 ± 0.77	-2.55 ± 1.65
Pocket2Mol	3.72 ± 0.68	2.59 ± 0.39	3.97 ± 0.44	4.78 ± 0.66	3.02 ± 0.41
PocketFlow	3.02 ± 0.65	0.57 ± 0.75	1.85 ± 0.54	4.40 ± 0.74	1.86 ± 0.88
ResGen	–	2.19 ± 0.32	0.77 ± 0.52	2.92 ± 0.32	–
3DSBDD	-0.19 ± 1.18	1.01 ± 0.75	-2.16 ± 0.76	0.56 ± 1.15	-2.56 ± 1.25

a): targets in CrossDocking

Model	7W7C	8JJL	7D42	7S1S	6AZV
SMILES-GA	0.91 ± 0.79	1.54 ± 0.60	1.03 ± 0.75	1.23 ± 0.65	1.28 ± 0.61
SMILES-LSTM-HC	3.39 ± 0.60	3.39 ± 0.60	3.39 ± 0.60	3.39 ± 0.60	3.39 ± 0.60
REINVENT	2.08 ± 0.53	2.16 ± 0.53	2.08 ± 0.50	2.21 ± 0.57	2.15 ± 0.50
Pasithea	2.50 ± 0.30	2.50 ± 0.30	2.50 ± 0.30	2.50 ± 0.30	2.50 ± 0.30
SMILES-VAE	2.54 ± 0.35	2.55 ± 0.40	2.57 ± 0.38	2.53 ± 0.39	2.47 ± 0.39
graph-GA	1.81 ± 0.62	1.58 ± 0.66	1.83 ± 0.55	1.69 ± 0.64	1.63 ± 0.62
MIMOSA	2.55 ± 0.38	2.55 ± 0.38	2.55 ± 0.38	2.55 ± 0.38	2.55 ± 0.38
MolDQN	-1.14 ± 0.68	-1.68 ± 0.70	-1.83 ± 0.68	-1.49 ± 0.69	-1.63 ± 0.75
DST	2.60 ± 0.28	2.57 ± 0.27	2.60 ± 0.28	2.60 ± 0.28	2.60 ± 0.28
JT-VAE	1.13 ± 0.92	2.28 ± 0.59	2.50 ± 0.50	2.28 ± 0.53	2.35 ± 0.56
TargetDiff	1.01 ± 1.35	-7.95 ± 20.45	-0.28 ± 0.00	–	–
Pocket2Mol	1.62 ± 0.58	3.43 ± 0.27	2.05 ± 0.70	1.35 ± 0.67	3.24 ± 0.56
PocketFlow	4.30 ± 0.52	2.52 ± 0.64	4.51 ± 0.46	-0.05 ± 0.64	5.24 ± 0.57
ResGen	1.63 ± 0.49	–	1.67 ± 0.39	1.62 ± 0.39	1.79 ± 0.36
3DSBDD	-11.36 ± 11.32	3.73 ± 1.18	0.04 ± 1.80	-3.82 ± 1.76	-0.32 ± 1.20

b): targets not in CrossDocking

Table 10: Top 100 LogP score for each target

Table 11: Top 1 QED score for each target. Targets in CrossDocking are marked in red, and targets not in CrossDocking are in blue.

Model	6GL8	1UWH	7OTE	1KKQ	5WFD	7W7C	8JJL	7D42	7S1S	6AZV
SMILES-GA	0.94	0.93	0.94	0.94	0.94	0.92	0.92	0.94	0.92	0.92
SMILES-LSTM-HC	0.94	0.94	0.94	0.94	0.94	0.94	0.94	0.94	0.94	0.94
REINVENT	0.95	0.95	0.95	0.95	0.95	0.95	0.95	0.95	0.95	0.95
Pasithea	0.95	0.95	0.94	0.94	0.94	0.94	0.94	0.94	0.94	0.94
SMILES-VAE	0.95	0.95	0.95	0.95	0.95	0.95	0.95	0.95	0.95	0.95
graph-GA	0.93	0.94	0.93	0.94	0.93	0.94	0.92	0.92	0.94	0.93
MIMOSA	0.95	0.95	0.95	0.95	0.95	0.95	0.95	0.95	0.95	0.95
MolDQN	0.65	0.75	0.58	0.63	0.59	0.55	0.66	0.53	0.72	0.55
DST	0.94	0.94	0.94	0.94	0.94	0.94	0.94	0.94	0.94	0.94
JT-VAE	0.94	0.94	0.94	0.94	0.94	0.94	0.94	0.94	0.94	0.94
TargetDiff	–	0.06	–	0.86	0.72	0.28	0.51	0.38	–	–
Pocket2Mol	0.95	0.94	0.94	0.94	0.93	0.94	0.93	0.89	0.94	0.94
PocketFlow	0.91	0.79	0.88	0.93	0.88	0.92	0.90	0.94	0.78	0.90
ResGen	–	0.78	0.65	0.93	–	0.70	–	0.89	0.93	0.89
3DSBDD	0.92	0.92	0.88	0.86	0.85	0.91	0.87	0.93	0.91	0.92

Model	6GL8	1UWH	7OTE	1KKQ	5WFD
SMILES-GA	0.92 ± 0.01	0.91 ± 0.01	0.92 ± 0.01	0.93 ± 0.01	0.92 ± 0.01
SMILES-LSTM-HC	0.93 ± 0.01	0.93 ± 0.01	0.93 ± 0.01	0.93 ± 0.01	0.93 ± 0.01
REINVENT	0.94 ± 0.01	0.93 ± 0.01	0.93 ± 0.01	0.94 ± 0.01	0.94 ± 0.01
Pasithea	0.94 ± 0.01	0.94 ± 0.01	0.94 ± 0.00	0.93 ± 0.00	0.94 ± 0.00
SMILES-VAE	0.94 ± 0.00	0.94 ± 0.00	0.94 ± 0.00	0.94 ± 0.01	0.94 ± 0.00
graph-GA	0.92 ± 0.01	0.91 ± 0.01	0.92 ± 0.01	0.91 ± 0.01	0.91 ± 0.01
MIMOSA	0.94 ± 0.00	0.94 ± 0.00	0.94 ± 0.00	0.94 ± 0.00	0.94 ± 0.00
MolDQN	0.60 ± 0.03	0.67 ± 0.03	0.54 ± 0.02	0.60 ± 0.02	0.53 ± 0.04
DST	0.94 ± 0.00	0.94 ± 0.00	0.94 ± 0.00	0.94 ± 0.00	0.94 ± 0.00
JT-VAE	0.93 ± 0.01	0.93 ± 0.01	0.93 ± 0.01	0.92 ± 0.01	0.93 ± 0.01
TargetDiff	–	0.06 ± 0.00	–	0.82 ± 0.02	0.56 ± 0.09
Pocket2Mol	0.93 ± 0.01	0.92 ± 0.01	0.93 ± 0.01	0.91 ± 0.02	0.91 ± 0.01
PocketFlow	0.90 ± 0.01	0.74 ± 0.03	0.83 ± 0.02	0.90 ± 0.02	0.85 ± 0.02
ResGen	–	0.74 ± 0.02	0.63 ± 0.01	0.91 ± 0.01	–
3DSBDD	0.90 ± 0.01	0.88 ± 0.02	0.82 ± 0.03	0.79 ± 0.03	0.79 ± 0.03

a): targets in CrossDocking

Model	7W7C	8JJL	7D42	7S1S	6AZV
SMILES-GA	0.91 ± 0.01	0.91 ± 0.01	0.92 ± 0.01	0.91 ± 0.01	0.91 ± 0.01
SMILES-LSTM-HC	0.93 ± 0.01	0.93 ± 0.01	0.93 ± 0.01	0.93 ± 0.01	0.93 ± 0.01
REINVENT	0.94 ± 0.01	0.93 ± 0.01	0.94 ± 0.01	0.93 ± 0.01	0.93 ± 0.01
Pasithea	0.94 ± 0.00	0.94 ± 0.00	0.94 ± 0.00	0.94 ± 0.00	0.94 ± 0.00
SMILES-VAE	0.94 ± 0.00	0.94 ± 0.00	0.94 ± 0.00	0.94 ± 0.00	0.94 ± 0.00
graph-GA	0.92 ± 0.01	0.90 ± 0.01	0.91 ± 0.01	0.91 ± 0.01	0.91 ± 0.01
MIMOSA	0.94 ± 0.00	0.94 ± 0.00	0.94 ± 0.00	0.94 ± 0.00	0.94 ± 0.00
MolDQN	0.52 ± 0.01	0.56 ± 0.04	0.50 ± 0.02	0.67 ± 0.03	0.52 ± 0.01
DST	0.94 ± 0.00	0.94 ± 0.00	0.94 ± 0.00	0.94 ± 0.00	0.94 ± 0.00
JT-VAE	0.91 ± 0.01	0.93 ± 0.01	0.92 ± 0.01	0.93 ± 0.01	0.93 ± 0.01
TargetDiff	0.17 ± 0.09	0.23 ± 0.18	0.38 ± 0.00	–	–
Pocket2Mol	0.93 ± 0.00	0.92 ± 0.01	0.87 ± 0.01	0.91 ± 0.01	0.93 ± 0.01
PocketFlow	0.89 ± 0.02	0.88 ± 0.01	0.87 ± 0.03	0.72 ± 0.03	0.88 ± 0.01
ResGen	0.67 ± 0.01	–	0.88 ± 0.01	0.91 ± 0.01	0.84 ± 0.02
3DSBDD	0.78 ± 0.06	0.79 ± 0.04	0.90 ± 0.02	0.85 ± 0.04	0.90 ± 0.02

b): targets not in CrossDocking

Table 12: Top 10 QED score for each target

Model	6GL8	1UWH	7OTE	1KKQ	5WFD
SMILES-GA	0.87 ± 0.03	0.87 ± 0.02	0.87 ± 0.03	0.86 ± 0.03	0.86 ± 0.03
SMILES-LSTM-HC	0.88 ± 0.03	0.88 ± 0.03	0.88 ± 0.03	0.88 ± 0.03	0.88 ± 0.03
REINVENT	0.89 ± 0.02	0.89 ± 0.02	0.89 ± 0.02	0.89 ± 0.02	0.90 ± 0.02
Pasithea	0.90 ± 0.02	0.90 ± 0.02	0.90 ± 0.02	0.90 ± 0.02	0.90 ± 0.02
SMILES-VAE	0.91 ± 0.01	0.91 ± 0.01	0.91 ± 0.02	0.89 ± 0.02	0.91 ± 0.02
graph-GA	0.84 ± 0.04	0.84 ± 0.04	0.84 ± 0.04	0.84 ± 0.04	0.84 ± 0.04
MIMOSA	0.91 ± 0.02	0.91 ± 0.02	0.91 ± 0.02	0.91 ± 0.02	0.91 ± 0.02
MolDQN	0.45 ± 0.06	0.49 ± 0.08	0.44 ± 0.05	0.47 ± 0.06	0.44 ± 0.05
DST	0.91 ± 0.02	0.90 ± 0.02	0.91 ± 0.02	0.91 ± 0.02	0.91 ± 0.02
JT-VAE	0.87 ± 0.03	0.88 ± 0.03	0.88 ± 0.02	0.88 ± 0.02	0.87 ± 0.03
TargetDiff	–	0.06 ± 0.00	–	0.66 ± 0.08	0.24 ± 0.17
Pocket2Mol	0.86 ± 0.04	0.81 ± 0.05	0.84 ± 0.05	0.75 ± 0.09	0.83 ± 0.05
PocketFlow	0.78 ± 0.06	0.62 ± 0.06	0.74 ± 0.05	0.79 ± 0.06	0.73 ± 0.06
ResGen	–	0.68 ± 0.03	0.58 ± 0.03	0.87 ± 0.02	–
3DSBDD	0.78 ± 0.06	0.76 ± 0.07	0.73 ± 0.05	0.64 ± 0.09	0.62 ± 0.08

a): targets in CrossDocking

Model	7W7C	8JJL	7D42	7S1S	6AZV
SMILES-GA	0.86 ± 0.03	0.86 ± 0.03	0.86 ± 0.03	0.86 ± 0.03	0.86 ± 0.03
SMILES-LSTM-HC	0.88 ± 0.03	0.88 ± 0.03	0.88 ± 0.03	0.88 ± 0.03	0.88 ± 0.03
REINVENT	0.89 ± 0.02	0.89 ± 0.02	0.89 ± 0.02	0.89 ± 0.02	0.89 ± 0.02
Pasithea	0.90 ± 0.02	0.90 ± 0.02	0.90 ± 0.02	0.90 ± 0.02	0.90 ± 0.02
SMILES-VAE	0.91 ± 0.02	0.91 ± 0.02	0.91 ± 0.02	0.91 ± 0.02	0.91 ± 0.02
graph-GA	0.84 ± 0.04	0.83 ± 0.04	0.84 ± 0.04	0.84 ± 0.04	0.83 ± 0.04
MIMOSA	0.91 ± 0.02	0.91 ± 0.02	0.91 ± 0.02	0.91 ± 0.02	0.91 ± 0.02
MolDQN	0.44 ± 0.04	0.45 ± 0.05	0.43 ± 0.03	0.49 ± 0.08	0.43 ± 0.04
DST	0.91 ± 0.02	0.90 ± 0.02	0.91 ± 0.02	0.91 ± 0.02	0.91 ± 0.02
JT-VAE	0.82 ± 0.05	0.88 ± 0.03	0.87 ± 0.02	0.88 ± 0.03	0.88 ± 0.03
TargetDiff	0.17 ± 0.09	0.23 ± 0.18	0.38 ± 0.00	–	–
Pocket2Mol	0.89 ± 0.03	0.87 ± 0.03	0.81 ± 0.03	0.83 ± 0.04	0.84 ± 0.05
PocketFlow	0.80 ± 0.05	0.79 ± 0.05	0.75 ± 0.06	0.60 ± 0.06	0.78 ± 0.05
ResGen	0.62 ± 0.03	–	0.80 ± 0.04	0.87 ± 0.02	0.78 ± 0.04
3DSBDD	0.49 ± 0.16	0.62 ± 0.07	0.75 ± 0.08	0.52 ± 0.18	0.73 ± 0.09

b): targets not in CrossDocking

Table 13: Top 100 QED score for each target

Table 14: Top 1 SA score for each target. Targets in CrossDocking are marked in red, and targets not in CrossDocking are in blue.

Model	6GL8	1UWH	7OTE	1KKQ	5WFD	7W7C	8JJL	7D42	7S1S	6AZV
SMILES-GA	1.65	1.65	1.65	1.65	1.65	1.65	1.65	1.65	1.65	1.65
SMILES-LSTM-HC	1.51	1.50	1.51	1.51	1.51	1.51	1.51	1.51	1.51	1.51
REINVENT	1.58	1.58	1.58	1.58	1.58	1.58	1.27	1.58	1.58	1.58
Pasithea	1.63	1.52	1.50	1.54	1.50	1.50	1.50	1.50	1.50	1.50
SMILES-VAE	1.44	1.50	1.50	1.50	1.50	1.50	1.44	1.50	1.50	1.50
graph-GA	1.00	1.00	1.00	1.00	1.00	1.00	1.00	1.00	1.00	1.00
MIMOSA	1.50	1.50	1.50	1.50	1.50	1.50	1.50	1.50	1.50	1.50
MolDQN	1.51	1.75	1.65	1.51	1.85	1.62	1.62	1.85	1.51	1.61
DST	1.50	1.50	1.50	1.50	1.50	1.50	1.50	1.50	1.50	1.50
JT-VAE	1.50	1.38	1.50	1.38	1.25	1.50	1.50	1.11	1.50	1.41
TargetDiff	–	4.05	–	1.76	2.96	3.86	3.68	3.41	–	–
Pocket2Mol	1.00	1.03	1.00	1.03	1.00	1.09	1.18	1.63	1.32	1.00
PocketFlow	1.00	1.00	1.00	1.00	1.00	1.00	1.00	1.00	1.61	1.00
ResGen	–	1.00	1.18	1.00	–	1.00	–	1.00	1.16	1.00
3DSBDD	1.00	1.20	2.03	1.84	1.00	3.07	1.21	1.55	1.88	1.00

Model	6GL8	1UWH	7OTE	1KKQ	5WFD
SMILES-GA	1.84 ± 0.10	1.87 ± 0.12	1.79 ± 0.08	1.87 ± 0.12	1.85 ± 0.11
SMILES-LSTM-HC	1.67 ± 0.07	1.66 ± 0.08	1.67 ± 0.07	1.67 ± 0.07	1.67 ± 0.07
REINVENT	1.72 ± 0.07	1.73 ± 0.07	1.74 ± 0.08	1.74 ± 0.08	1.74 ± 0.08
Pasithea	1.73 ± 0.05	1.70 ± 0.11	1.66 ± 0.09	1.67 ± 0.07	1.66 ± 0.09
SMILES-VAE	1.64 ± 0.10	1.67 ± 0.07	1.67 ± 0.08	1.64 ± 0.10	1.64 ± 0.08
graph-GA	1.24 ± 0.25	1.07 ± 0.09	1.35 ± 0.24	1.12 ± 0.13	1.08 ± 0.05
MIMOSA	1.70 ± 0.08	1.70 ± 0.08	1.70 ± 0.08	1.70 ± 0.08	1.70 ± 0.08
MolDQN	1.84 ± 0.14	2.09 ± 0.19	1.90 ± 0.18	1.83 ± 0.14	2.02 ± 0.15
DST	1.66 ± 0.09	1.66 ± 0.09	1.66 ± 0.09	1.66 ± 0.09	1.66 ± 0.09
JT-VAE	1.81 ± 0.12	1.71 ± 0.15	1.67 ± 0.09	1.65 ± 0.13	1.64 ± 0.17
TargetDiff	–	4.05 ± 0.00	–	2.41 ± 0.27	3.54 ± 0.28
Pocket2Mol	1.20 ± 0.13	1.50 ± 0.22	1.10 ± 0.08	1.45 ± 0.20	1.05 ± 0.06
PocketFlow	1.00 ± 0.00	1.37 ± 0.26	1.00 ± 0.00	1.07 ± 0.06	1.11 ± 0.10
ResGen	–	1.00 ± 0.00	1.40 ± 0.12	1.05 ± 0.06	–
3DSBDD	1.44 ± 0.25	1.47 ± 0.16	2.92 ± 0.41	2.90 ± 0.39	2.02 ± 0.59

a): targets in CrossDocking

Model	7W7C	8JJL	7D42	7S1S	6AZV
SMILES-GA	1.89 ± 0.14	1.85 ± 0.11	1.87 ± 0.11	1.86 ± 0.11	1.85 ± 0.09
SMILES-LSTM-HC	1.67 ± 0.07	1.67 ± 0.07	1.67 ± 0.07	1.67 ± 0.07	1.67 ± 0.07
REINVENT	1.74 ± 0.08	1.67 ± 0.15	1.74 ± 0.08	1.73 ± 0.07	1.73 ± 0.08
Pasithea	1.66 ± 0.09	1.66 ± 0.09	1.66 ± 0.09	1.66 ± 0.09	1.66 ± 0.09
SMILES-VAE	1.71 ± 0.09	1.64 ± 0.10	1.65 ± 0.07	1.67 ± 0.09	1.70 ± 0.08
graph-GA	1.12 ± 0.14	1.30 ± 0.21	1.14 ± 0.18	1.15 ± 0.16	1.31 ± 0.25
MIMOSA	1.70 ± 0.08	1.70 ± 0.08	1.70 ± 0.08	1.70 ± 0.08	1.70 ± 0.08
MolDQN	1.85 ± 0.16	2.01 ± 0.27	2.08 ± 0.20	1.92 ± 0.18	1.96 ± 0.20
DST	1.66 ± 0.09	1.66 ± 0.09	1.66 ± 0.09	1.66 ± 0.09	1.66 ± 0.09
JT-VAE	1.88 ± 0.13	1.83 ± 0.14	1.70 ± 0.24	1.78 ± 0.16	1.60 ± 0.10
TargetDiff	4.59 ± 0.67	5.23 ± 0.86	3.41 ± 0.00	–	–
Pocket2Mol	1.29 ± 0.13	1.36 ± 0.12	2.10 ± 0.22	1.78 ± 0.29	1.54 ± 0.22
PocketFlow	1.10 ± 0.08	1.16 ± 0.09	1.00 ± 0.00	1.77 ± 0.08	1.00 ± 0.00
ResGen	1.15 ± 0.11	–	1.14 ± 0.10	1.43 ± 0.11	1.05 ± 0.06
3DSBDD	4.40 ± 0.57	2.76 ± 0.76	1.98 ± 0.27	2.65 ± 0.48	1.80 ± 0.41

b): targets not in CrossDocking

Table 15: Top 10 SA score for each target

Model	6GL8	1UWH	7OTE	1KKQ	5WFD
SMILES-GA	2.55 ± 0.35	2.50 ± 0.33	2.53 ± 0.37	2.77 ± 0.49	2.52 ± 0.37
SMILES-LSTM-HC	1.93 ± 0.13	1.95 ± 0.14	1.93 ± 0.13	1.93 ± 0.13	1.93 ± 0.13
REINVENT	2.14 ± 0.20	2.14 ± 0.19	2.14 ± 0.19	2.15 ± 0.19	2.14 ± 0.18
Pasithea	2.01 ± 0.14	2.00 ± 0.14	1.97 ± 0.15	1.97 ± 0.14	1.96 ± 0.15
SMILES-VAE	1.96 ± 0.14	1.94 ± 0.13	1.96 ± 0.14	2.02 ± 0.17	1.96 ± 0.15
graph-GA	2.10 ± 0.36	1.94 ± 0.39	2.15 ± 0.37	1.94 ± 0.35	1.96 ± 0.43
MIMOSA	1.95 ± 0.12	1.95 ± 0.12	1.95 ± 0.12	1.95 ± 0.12	1.95 ± 0.12
MolDQN	2.93 ± 0.57	3.21 ± 0.51	2.98 ± 0.50	2.83 ± 0.53	3.15 ± 0.53
DST	1.95 ± 0.14	1.96 ± 0.14	1.95 ± 0.14	1.95 ± 0.14	1.95 ± 0.14
JT-VAE	2.29 ± 0.25	2.19 ± 0.22	2.21 ± 0.24	2.21 ± 0.25	2.23 ± 0.27
TargetDiff	–	4.05 ± 0.00	–	3.42 ± 0.48	4.50 ± 0.63
Pocket2Mol	1.69 ± 0.25	2.07 ± 0.29	1.92 ± 0.37	2.05 ± 0.29	1.43 ± 0.18
PocketFlow	1.36 ± 0.22	1.98 ± 0.30	1.30 ± 0.23	1.60 ± 0.29	1.86 ± 0.34
ResGen	–	1.29 ± 0.17	1.87 ± 0.25	1.49 ± 0.21	–
3DSBDD	3.00 ± 0.74	2.89 ± 0.73	4.39 ± 0.65	4.20 ± 0.61	4.40 ± 1.03

a): targets in CrossDocking

Model	7W7C	8JJL	7D42	7S1S	6AZV
SMILES-GA	2.77 ± 0.48	2.48 ± 0.32	2.66 ± 0.43	2.53 ± 0.35	2.55 ± 0.38
SMILES-LSTM-HC	1.93 ± 0.13	1.93 ± 0.13	1.93 ± 0.13	1.93 ± 0.13	1.93 ± 0.13
REINVENT	2.16 ± 0.20	2.14 ± 0.23	2.16 ± 0.19	2.11 ± 0.18	2.13 ± 0.19
Pasithea	1.97 ± 0.15	1.97 ± 0.15	1.97 ± 0.15	1.97 ± 0.15	1.97 ± 0.15
SMILES-VAE	1.99 ± 0.13	1.95 ± 0.14	1.95 ± 0.14	1.97 ± 0.13	1.96 ± 0.13
graph-GA	1.97 ± 0.37	2.15 ± 0.38	2.00 ± 0.37	2.01 ± 0.38	2.13 ± 0.35
MIMOSA	1.95 ± 0.12	1.95 ± 0.12	1.95 ± 0.12	1.95 ± 0.12	1.95 ± 0.12
MolDQN	3.05 ± 0.53	3.24 ± 0.55	3.28 ± 0.53	3.05 ± 0.53	3.14 ± 0.51
DST	1.95 ± 0.14	1.96 ± 0.14	1.95 ± 0.14	1.95 ± 0.14	1.95 ± 0.14
JT-VAE	2.64 ± 0.43	2.30 ± 0.22	2.23 ± 0.25	2.30 ± 0.26	2.18 ± 0.26
TargetDiff	4.59 ± 0.67	5.23 ± 0.86	3.41 ± 0.00	–	–
Pocket2Mol	2.05 ± 0.35	2.19 ± 0.39	2.72 ± 0.28	2.57 ± 0.39	2.14 ± 0.29
PocketFlow	1.71 ± 0.30	1.62 ± 0.26	1.17 ± 0.21	2.02 ± 0.10	1.06 ± 0.09
ResGen	1.76 ± 0.35	–	1.63 ± 0.24	1.86 ± 0.21	1.47 ± 0.21
3DSBDD	6.10 ± 0.96	4.89 ± 0.88	3.73 ± 0.90	4.87 ± 1.05	3.57 ± 0.83

b): targets not in CrossDocking

Table 16: Top 100 SA score for each target

Table 17: Posebusters evaluation results across models. The values represent the success rate of generated molecules for all receptor targets, indicating the proportion of molecules that meet the Posebusters validation criteria

Model	All Atoms Connected	Aromatic Ring Flatness	Bond Angles	Bond Lengths	Double Bond Flatness	Inchi Convertible
Pocket2Mol	0.763	0.990	0.989	0.988	0.970	0.559
PocketFlow	0.936	0.991	0.990	0.989	0.991	0.880
ResGen	0.947	0.988	0.989	0.989	0.987	0.913
3DSBDD	0.459	0.957	0.943	0.944	0.922	0.400
DST	1.000	1.000	1.000	0.999	1.000	1.000
graph-GA	1.000	1.000	1.000	0.999	1.000	1.000
JT-VAE	1.000	1.000	1.000	0.998	1.000	1.000
MIMOSA	1.000	1.000	1.000	0.999	1.000	1.000
MolDQN	1.000	1.000	0.968	0.950	0.998	1.000
Pasithea	0.956	0.767	0.766	0.765	0.767	0.738
REINVENT	0.915	0.803	0.802	0.802	0.803	0.733
SMILES-GA	0.954	0.720	0.719	0.719	0.719	0.699
SMILES-LSTM-HC	0.930	0.902	0.900	0.899	0.902	0.839
SMILES-VAE	0.959	0.776	0.776	0.775	0.776	0.745
TargetDiff	1.000	1.000	0.758	0.903	1.000	0.998

Model	Internal Energy	Internal Steric Clash	Min Dist To Inorg Cofactors	Min Dist To Org Cofactors	Min Dist To Protein	Min Dist To Waters
Pocket2Mol	0.471	0.968	1.000	1.000	0.935	1.000
PocketFlow	0.724	0.980	1.000	1.000	0.998	1.000
ResGen	0.711	0.983	1.000	1.000	1.000	1.000
3DSBDD	0.323	0.909	1.000	1.000	0.867	1.000
DST	0.972	1.000	1.000	1.000	0.996	1.000
graph-GA	0.970	0.999	1.000	1.000	0.998	1.000
JT-VAE	0.958	0.999	1.000	1.000	0.991	1.000
MIMOSA	0.968	1.000	1.000	1.000	0.997	1.000
MolDQN	0.947	0.990	1.000	1.000	1.000	1.000
Pasithea	0.724	0.763	1.000	1.000	0.996	1.000
REINVENT	0.717	0.800	1.000	1.000	0.998	1.000
SMILES-GA	0.678	0.714	1.000	1.000	0.998	1.000
SMILES-LSTM-HC	0.815	0.898	1.000	1.000	0.986	1.000
SMILES-VAE	0.735	0.775	1.000	1.000	0.997	1.000
TargetDiff	0.746	0.933	1.000	1.000	0.470	1.000

Model	Mol Cond Loaded	Mol Pred Loaded	Prot-Lig Max Dist	Sanitization	Vol Overlap w/ Inorg Cof	Vol Overlap w/ Org Cof	Vol Overlap w/ Protein
Pocket2Mol	1.000	1.000	1.000	0.992	1.000	1.000	1.000
PocketFlow	1.000	1.000	1.000	0.991	1.000	1.000	1.000
ResGen	1.000	1.000	1.000	0.989	1.000	1.000	1.000
3DSBDD	1.000	1.000	1.000	0.957	1.000	1.000	1.000
DST	1.000	1.000	1.000	1.000	1.000	1.000	1.000
graph-GA	1.000	1.000	1.000	1.000	1.000	1.000	1.000
JT-VAE	1.000	1.000	1.000	1.000	1.000	1.000	1.000
MIMOSA	1.000	1.000	1.000	1.000	1.000	1.000	1.000
MolDQN	1.000	1.000	1.000	1.000	1.000	1.000	0.996
Pasithea	1.000	1.000	1.000	0.767	1.000	1.000	1.000
REINVENT	1.000	1.000	1.000	0.803	1.000	1.000	1.000
SMILES-GA	1.000	1.000	1.000	0.720	1.000	1.000	1.000
SMILES-LSTM-HC	1.000	1.000	1.000	0.902	1.000	1.000	1.000
SMILES-VAE	1.000	1.000	1.000	0.776	1.000	1.000	1.000
TargetDiff	1.000	1.000	1.000	0.998	1.000	1.000	0.903

Table 18: Clash statistics across different models. An empty item (–) means the model either did not generate molecules for that target or the evaluation failed. UQ stands for Upper Quartile.

	6GL8				1UWH				7OTE				1KKQ				5WFD			
Model	Min	Max	Mean	UQ	Min	Max	Mean	UQ	Min	Max	Mean	UQ	Min	Max	Mean	UQ	Min	Max	Mean	UQ
DST	0	14	3.14	4	0	23	5.54	7	0	19	5.29	7	0	17	4.14	6	0	11	3.44	5
JT-VAE	0	14	3.56	5	0	60	6.28	8	0	30	6.44	9	0	21	4.96	6	0	16	4.00	5
MIMOSA	0	11	3.15	4	0	21	5.35	7	0	22	5.62	8	0	16	4.09	6	0	12	3.46	5
MolDQN	0	13	2.74	4	0	13	2.78	4	0	19	3.14	4	0	9	2.39	3	0	13	3.03	4
graph-GA	0	15	2.34	3	0	25	3.34	5	0	20	4.88	7	0	13	2.59	4	0	11	2.24	3
Pasithea	0	12	3.02	4	0	26	5.58	7	0	23	5.51	7	0	20	4.17	6	0	11	3.41	5
REINVENT	0	13	3.09	4	0	21	4.42	6	0	20	4.42	6	0	18	4.02	5	0	14	3.32	4
SMILES-GA	0	13	3.34	4	0	18	5.15	7	0	21	4.89	7	0	16	4.12	5	0	10	3.57	5
SMILES-LSTM-HC	0	14	3.56	5	0	38	6.38	8	0	29	6.48	8	0	27	5.02	7	0	16	4.04	5
SMILES-VAE	0	9	2.93	4	0	25	5.45	7	0	22	5.41	7	0	17	4.01	5	0	10	3.42	5
3DSBDD	0	11	3.31	5	0	15	5.06	7	0	28	8.85	12	0	15	5.79	7	–	–	–	–
Pocket2Mol	0	15	4.14	5	0	49	9.09	12	0	34	8.28	11	0	27	7.73	10	0	15	4.30	6
PocketFlow	0	14	2.72	4	0	19	2.73	4	0	19	3.26	5	0	17	3.11	5	0	18	3.74	5
ResGen	–	–	–	–	0	9	2.32	3	0	8	1.61	2	0	16	5.34	7	–	–	–	–
TargetDiff	–	–	–	–	88	88	88.00	88	–	–	–	–	3	115	30.43	40	19	93	48.75	61

	7W7C				8JJL				7D42				7S1S				6AZV			
Model	Min	Max	Mean	UQ	Min	Max	Mean	UQ	Min	Max	Mean	UQ	Min	Max	Mean	UQ	Min	Max	Mean	UQ
DST	0	25	4.13	6	0	39	10.26	13	0	28	4.86	6	0	21	5.49	7	0	19	4.87	6
JT-VAE	0	47	5.69	7	0	74	13.87	18	0	66	7.15	9	0	25	6.78	9	0	21	5.37	7
MIMOSA	0	27	4.23	6	0	47	10.33	13	0	38	4.68	6	0	25	5.46	7	0	18	4.83	6
MolDQN	0	9	1.77	3	0	20	4.03	5	0	13	2.26	3	0	15	3.46	5	0	12	2.33	3
graph-GA	0	29	2.57	3	0	51	9.04	13	0	33	2.91	3	0	16	3.35	4	0	19	2.73	4
Pasithea	0	33	4.14	5	0	52	10.28	14	0	30	5.01	6	0	20	5.26	7	0	22	4.62	6
REINVENT	0	32	4.18	6	0	36	7.81	10	0	36	4.91	6	0	27	5.52	7	0	21	4.68	6
SMILES-GA	0	25	4.46	6	0	31	9.82	13	0	22	4.33	6	0	18	5.25	7	0	17	4.79	7
SMILES-LSTM-HC	0	69	6.99	9	0	98	15.51	19	0	88	8.81	11	0	28	6.42	8	0	20	5.22	7
SMILES-VAE	0	30	4.14	6	0	40	10.06	13	0	26	4.66	6	0	17	5.27	7	0	19	4.82	6
3DSBDD	–	–	–	–	–	–	–	–	0	12	5.19	7	0	20	7.20	9	0	44	8.10	11
Pocket2Mol	0	64	8.67	9	0	103	20.42	26	0	84	23.82	33	0	34	7.48	10	0	21	6.56	9
PocketFlow	0	26	5.75	9	0	48	8.64	13	0	64	8.09	11	0	23	4.82	6	0	20	4.33	6
ResGen	0	6	1.64	2	–	–	–	–	0	14	3.41	5	0	16	4.70	6	0	20	4.09	6
TargetDiff	140	173	160.00	170	61	176	112.90	130	51	51	51.00	51	–	–	–	–	–	–	–	–